Inorg. Chem. **2003**, *42*, 3801–3814

Cationic Carbonyl Complexes of Rhodium(I) and Rhodium(III): Syntheses, Vibrational Spectra, NMR Studies, and Molecular Structures of Tetrakis(carbonyl)rhodium(I) Heptachlorodialuminate and -gallate, $[Rh(CO)_4][Al_2Cl_7]$ and $[Rh(CO)_4][Ga_2Cl_7]$

Britta von Ahsen,[†] Christian Bach,[†] Michael Berkei,[†] Martin Köckerling,[†] Helge Willner,*[,†] Gerhard Hägele,[‡] and Friedhelm Aubke*[,§]

Fakultät 4, Anorganische Chemie, Gerhard Mercator Universität Duisburg, Lotharstrasse 1, D-47048 Duisburg, Germany, Anorganische Chemie und Strukturchemie, Heinrich Heine Universität Düsseldorf, Universitätsstrasse 1, D-40225 Düsseldorf, Germany, and Department of Chemistry, The University of British Columbia, 2036 Main Mall, Vancouver, BC V6T1Z1, Canada

Received November 26, 2002

Dimeric rhodium(I) bis(carbonyl) chloride, $[Rh(CO)_2(\mu\text{-}Cl)]_2$, is found to be a useful and convenient starting material for the syntheses of new cationic carbonyl complexes of both rhodium(I) and rhodium(III). Its reaction with the Lewis acids $AlCl_3$ or $GaCl_3$ produces in a CO atmosphere at room temperature the salts $[Rh(CO)_4][M_2Cl_7]$ (M = Al, Ga), which are characterized by Raman spectroscopy and single-crystal X-ray diffraction. Crystal data for $[Rh(CO)_4][Al_2Cl_7]$: triclinic, space group $P\bar{1}$ (No. 2); $a = 9.705(3)$, $b = 9.800(2)$, $c = 10.268(2)$ Å; $\alpha = 76.52(2)$, $\beta = 76.05(2)$, $\gamma = 66.15(2)°$; $V = 856.7(5)$ Å^3; $Z = 2$; $T = 293$ K; R_1 [$I > 2\sigma(I)$] = 0.0524, $wR_2 = 0.1586$. Crystal data for $[Rh(CO)_4][Ga_2Cl_7]$: triclinic, space group $P\bar{1}$ (No. 2); $a = 9.649(1)$, $b = 9.624(1)$, $c = 10.133(1)$ Å; $\alpha = 77.38(1)$, $\beta = 76.13(1)$, $\gamma = 65.61(1)°$; $V = 824.4(2)$ Å^3; $Z = 2$; $T = 143$ K; R_1 [$I > 2\sigma(I)$] = 0.0358, $wR_2 = 0.0792$. Structural parameters for the square planar cation $[Rh(CO)_4]^+$ are compared to those of isoelectronic $[Pd(CO)_4]^{2+}$ and of $[Pt(CO)_4]^{2+}$. Dissolution of $[Rh(CO)_2Cl]_2$ in HSO_3F in a CO atmosphere allows formation of $[Rh(CO)_4]^+_{(solv)}$. Oxidation of $[Rh(CO)_2Cl]_2$ by $S_2O_6F_2$ in HSO_3F results in the formation of $ClOSO_2F$ and two seemingly oligomeric Rh(III) carbonyl fluorosulfato intermediates, which are easily reduced by CO addition to $[Rh(CO)_4]^+_{(solv)}$. Controlled oxidation of this solution with $S_2O_6F_2$ produces *fac*-$Rh(CO)_3(SO_3F)_3$ in about 95% yield. This Rh(III) complex can be reduced by CO at 25 °C in anhydrous HF to give $[Rh(CO)_4]^+_{(solv)}$; addition of SbF_5 at –40 °C to the resulting solution allows isolation of $[Rh(CO)_4][Sb_2F_{11}]$, which is found to have a highly symmetrical (D_{4h}) $[Sb_2F_{11}]^-$ anion. Oxidation of $[Rh(CO)_2Cl]_2$ in anhydrous HF by F_2, followed in a second step by carbonylation in the presence of SbF_5, is found to be a simple, straightforward route to pure $[Rh(CO)_5Cl][Sb_2F_{11}]_2$, which has previously been structurally characterized by us. All new complexes are characterized by vibrational and NMR spectroscopy. Assignment of the vibrational spectra and interpretation of the structural data are supported by DFT calculations.

Introduction

Thermally stable σ-bonded metal carbonyl cations[1–3] and their derivatives are a very recent addition to the large and diverse metal carbonyl family.[4–10] The use of superacids[11,12] like $HF-SbF_5$[13,14] as reaction media and the development of useful synthetic routes[2,3] have allowed us to generate σ-carbonyl cations and their derivatives for 16 metals, ranging from group 12 (Hg) to group 6 (W, Mo).[1–3] Salts are formed with the superacid anions $[Sb_2F_{11}]^-$ and $[SbF_6]^-$.[15]

* To whom correspondence should be addressed. E-mail: willner@uni-duisburg.de (H.W.); aubke@chem.ubc.ca (F.A.). Phone: int. 49-203-379-3309 (H.W.); int. 604-822-3817 (F.A.). Fax: int. 49-203-379-2231 (H.W.); int. 604-822-2847 (F.A.).

[†] Gerhard Mercator Universität Duisburg.

[‡] Heinrich Heine Universität Düsseldorf.

[§] The University of British Columbia.

(1) Willner, H.; Aubke, F. *Angew. Chem., Int. Ed. Engl.* **1997**, *36*, 2402.

(2) Willner, H.; Aubke, F. In *Inorganic Chemistry Highlights*; Meyer, G., Naumann, D., Wesemann, L., Eds.; Wiley-VCH: Weinheim, Germany, 2002; p 195.

(3) Willner, H.; Aubke, F. *Chem.—Eur. J.* **2003**, *9*, in press.

10.1021/ic0206903 CCC: $25.00
Published on Web 05/14/2003

A substantial number of these salts have been structurally characterized.[2,3]

The metals in group 9 present a serious challenge to our synthetic approach.[1−3] Of the univalent cations $[M(CO)_4]^+$ (M = Rh, Ir), which are expected to be square planar with a d^8 electron configuration, only for Rh(I) a salt of the type $[Rh(CO)_4][1\text{-Et-}CB_{11}F_{11}]$ has recently been obtained and is structurally characterized.[16] For Co(I), salts with a homoleptic metal carbonyl cation have been unknown until very recently. $[Co(CO)_4]^+_{(solv)}$ is claimed to exist in strong protonic acids such as H_2SO_4, HSO_3F, etc.[17] The use of a new conjugate Brønsted−Lewis superacid system formed by the Brønsted acid[11,12] HF and the nonoxidizing krypto Lewis acid $(CF_3)_3$-BCO[17a] has allowed the isolation of $[Co(CO)_5][FB(CF_3)_3]$,[17b] which is structurally characterized. The trigonal bypyramidal $[Co(CO)_5]^+$ is unprecedented among known homoleptic metal carbonyl cations.[1−3] Oxidative interference from SbF_5 had previously curtailed all attempts to generate unipositive, oxidatively sensitive cations of the type $[M(CO)_n]^+$ ($n = 4$, 5), with M = Co, Rh, and Ir, in HF−SbF_5.

On the other hand, the generation of cationic, structurally characterized Ir(III) carbonyl complexes has been rather successful.[1−3] The addition of CO to $Ir(SO_3F)_3$[18] in HSO_3F results in the formation of *mer*-$Ir(CO)_3(SO_3F)_3$ as the main product.[19] The reaction of this compound with SbF_5 in a CO atmosphere and traces of halocarbon grease produces unexpectedly $[Ir(CO)_5Cl][Sb_2F_{11}]_2$.[20] A more straightforward synthesis of this compound by the oxidative carbonylation of $[Ir(CO)_3Cl]_x$ has subsequently been reported.[21] Finally, $[Ir(CO)_6]^{3+}$ is generated by the reductive carbonylation of IrF_6.[20,22,23] In SbF_5, the polycrystalline salt $[Ir(CO)_6][Sb_2F_{11}]_3$ is isolated,[20,21] while, from a dilute solution of SbF_5 in HF, single crystals of the solvate $[Ir(CO)_6][SbF_6]_3\cdot 4HF$ are obtained.[23]

To synthesize the corresponding Rh(III) carbonyl compounds, an approach different from the one used for the syntheses of iridium(III) cationic carbonyl complexes[19−23] is needed, because Rh(III) is easily reduced by CO to Rh(I). Although $Rh(SO_3F)_3$ is known, it is exceedingly difficult to synthesize.[24] Likewise RhF_6[25] is not as easily obtained as IrF_6[26,27] and appears to be a far more powerful oxidizer than IrF_6. So far only $[Rh(CO)_5Cl][Sb_2F_{11}]_2$ is known.[21] While the molecular structure is obtained,[21] its synthesis by oxidative carbonylation of $[Rh(CO)_2Cl]_2$ with SbF_5 as oxidizer produces the adduct $6SbF_3\cdot 5SbF_5$[28] as an inseparable byproduct.

The first evidence for $[Rh(CO)_4]^+_{(solv)}$ is obtained by Raman spectroscopy. In HSO_3F solution, $[Rh(CO)_4]^+_{(solv)}$ is formed by reduction of small amounts of $Rh(SO_3F)_3$[24] with CO[29] or by addition of CO to $[Rh(CO)_2Cl]_2$.[30] Since the solutions are found to be unstable, a solid product is not isolated.

The message contained in this brief summary is 2-fold:

(i) Judging by existing precedents[16,17] and references cited there, salts with the $[Rh(CO)_4]^+$ cation are obtainable, as long as nonoxidizing Lewis acids are used in their generation or by selecting a specific synthetic approach to $[Rh(CO)_4][Sb_2F_{11}]$, where the oxidizing ability of SbF_5 is negated.

(ii) To generate cationic Rh(III) carbonyl complexes, the oxidation of suitable Rh(I) precursors by strong oxidizing agents should be more promising than the opposite approach, which is the reductive carbonylation of higher valent rhodium species to Rh(III) carbonyls.

There is an unique opportunity to synthesize and characterize cationic carbonyl complexes of rhodium, with the metal in two distinctly different oxidation states and coordination geometries: square planar Rh(I) (d^8); octahedral Rh(III) (d^6). It appears possible to establish a viable redox chemistry in superacid media,[11,12] involving well-defined mononuclear carbonyl derivatives. This is not possible for other mononuclear metal carbonyl cations and their derivatives, which are only known with the metal in a single oxidation state.[1−3] Even for iridium, where an extensive amount of work is reported on octahedral Ir(III) carbonyl complexes,[19−23] there is at present only very preliminary Raman spectroscopic evidence for $[Ir(CO)_4]^+$ in molten $AlCl_3$ under a CO atmosphere.[30,31]

(4) Lupinetti, A. J.; Frenking, G.; Strauss, S. H. *Prog. Inorg. Chem.* **2000**, *49*, 1.
(5) Ellis, J. E. *Adv. Organomet. Chem.* **1990**, *31*, 1.
(6) Cotton, F. A.; Wilkinson, G. In *Advanced Inorganic Chemistry*, 5th ed.; Wiley: New York, 1988; p 58.
(7) Pruchnik, F. P. *Organometallic Chemistry of Transition Elements*; Plenum Press: New York, 1990.
(8) Elschenbroich, C.; Salzer, A. *Organometallics*; VCH: Weinheim, Germany, 1992.
(9) Crabtree, R. M. In *The Organometallic Chemistry of the Transition Metals*, 2nd ed.; Wiley: New York, 1994; p 142.
(10) Werner, H. *Angew. Chem., Int. Ed. Engl.* **1990**, *29*, 1077.
(11) Olah, G. A.; Prakash, G. K. S.; Sommer, J. *Superacids*; Wiley: New York, 1985.
(12) O'Donell, T. A. *Superacids and Acidic Melts as Inorganic Reaction Media*; VCH: Weinheim, Germany, 1993.
(13) Hyman, H. M.; Quaterman, L.; Kirkpatrick, M.; Katz, J. J. *J. Phys. Chem.* **1961**, *65*, 123.
(14) Gillespie, R. J.; Moss, K. C. *J. Chem. Soc. A* **1966**, 1170.
(15) Zhang, D.; Rettig, S. J.; Trotter, J.; Aubke, F. *Inorg. Chem.* **1996**, *35*, 6113.
(16) Lupinetti, A. J.; Havighurst, M. D.; Miller, S. M.; Anderson, O. P.; Strauss, S. H. *J. Am. Chem. Soc.* **1999**, *121*, 11920.
(17) Xu, Q.; Inoue, S.; Souma, Y.; Nakatani, H. *J. Organomet. Chem.* **2000**, *606*, 147. (a) Finze, M.; Bernhardt, E.; Terheiden, A.; Berkei, M.; Willner, H.; Christen, D.; Oberhammer, H.; Aubke, F. *J. Am. Chem. Soc.* **2002**, *124*, 15385. (b) Willner, H.; Bernhardt, E.; Finze, M.; Lehmann, C. W.; Aubke, F. *Angew. Chem.*, accepted for publication.
(18) Lee, K. C.; Aubke, F. *J. Fluorine Chem.* **1982**, *19*, 501.
(19) Wang, C.; Lewis, A. R.; Batchelor, R. J.; Einstein, F. W. B.; Willner, H.; Aubke, F. *Inorg. Chem.* **1996**, *35*, 1279.
(20) Bach, C.; Willner, H.; Wang, C.; Rettig, S. J.; Trotter, J.; Aubke, F. *Angew. Chem., Int. Ed. Engl.* **1996**, *35*, 1974.
(21) Willner, H.; Bach, C.; Wartchow, R.; Wang, C.; Rettig, S. J.; Trotter, J.; Jonas, V.; Thiel, W.; Aubke, F. *Inorg. Chem.* **2000**, *39*, 1933.
(22) v. Ahsen, B.; Bach, C.; Pernice, H.; Willner, H.; Aubke, F. *J. Fluorine Chem.* **2000**, *102*, 243.
(23) v. Ahsen, B.; Berkei, M.; Henkel, G.; Willner, H.; Aubke, F. *J. Am. Chem. Soc.* **2002**, *124*, 8371.
(24) Leung, P. C.; Wong, G.; Aubke, F. *J. Fluorine Chem.* **1987**, *35*, 607.
(25) Chernick, C. L.; Classen, H. H.; Weinstock, B. *J. Am. Chem. Soc.* **1961**, *83*, 3165.
(26) Ruff, O.; Fischer, J. *Z. Anorg. Allg. Chem.* **1929**, *179*, 166.
(27) Hargreaves, G. B.; Peacock, R. D. *Proc. Chem. Soc. London* **1959**, 85.
(28) Nandana, W. A. S.; Passmore, J.; White, P. S. *J. Chem. Soc., Dalton Trans.* **1985**, 1623.
(29) Wang, C. Ph.D. Thesis, University of British Columbia, 1996.
(30) Bach, C. Ph.D. Thesis, Universität Hannover, 1999.
(31) Willner, H.; Bodenbinder, M.; Bröchler, R.; Hwang, G.; Rettig, S. J.; Trotter, J.; v. Ahsen, B.; Westphal, U.; Jonas, V.; Thiel, W.; Aubke, F. *J. Am. Chem. Soc.* **2001**, *123*, 588.

Experimental Section

(a) Chemicals. $[Rh(CO)_2Cl]_2$ (99% purity) and $AlCl_3$ (99.9% purity) both from Chempur, Karlsruhe, Germany, were used without further purification. Gallium trichloride was synthesized by the reaction of gallium metal (99.99% purity; Strem Chemicals Inc., Kehl, Germany) with chlorine (technical grade) in a sealed glass reactor at room temperature, with a Cl_2 pressure of about 6 atm. The product was purified by sublimation in vacuo (10^{-5} mbar) at 40 °C. F_2 (technical grade, Solvay, Hanover, Germany), HSO_3F (technical grade, Bayer AG, Leverkusen, Germany), and SbF_5 (Scientific Industrial Association, Moscow, Russia) were used. The latter two were purified by distillation first at atmospheric pressure and then in vacuo. Anhydrous HF (99% purity; Allied Signal, Seelze, Germany) was used without further purification and stored over a small amount of SbF_5 to remove traces of water as $[H_3O][Sb_2F_{11}]$.[15] Bis(fluorosulfuryl) peroxide, $S_2O_6F_2$,[32] was synthesized by the catalytic (AgF_2) fluorination of SO_3 (Dupont) with elemental fluorine, as described.[33] Carbon monoxide (99%, Linde Gas, Hanover, Germany) was purified, by liquefying and evaporation of CO at −196 °C. ^{13}CO (99% enriched; Deutero GmbH, Kastellaun, Germany) was used without further purification.

Warning! *Of the chemicals used in this study F_2, $S_2O_6F_2$, SO_3, Cl_2, and SbF_5 are strongly oxidizing, while HF, HSO_3F, and HF−SbF_5 are highly corrosive. Most of these and CO are toxic. All work should be done in well-ventilated fumehoods, with personal safety equipment in place.*

(b) Apparatus. Volatile materials were manipulated in a glass or stainless steel vacuum line of known volume, equipped with a capacitance pressure gauge (type 280E, Setra Instruments, Acton, MA) and valves with PTFE stems (Young, London) or stainless steel needle valves (3762H46Y Hoke, Creskill, NJ), respectively. Anhydrous HF, containing a few mole percent of SbF_5, was stored in a PFA tube (12 mm o.d., 300 mm long), which was heat sealed at the bottom and connected on top to a stainless steel needle valve (3762H46Y Hoke, Creskill, NJ). All other volatile reactants were stored in glass containers, equipped with a valve with PTFE stem (Young, London). In the case of ^{13}CO, the storage vessel contained a molecular sieve (5 Å, Merck) to recover the excess of ^{13}CO after use by cooling with liquid nitrogen. For synthetic reactions in HF/SbF_5 solutions, a two part V-shaped reactor with an approximate volume of 25 mL, consisting of two PFA tubes (12 mm o.d., 100 mm length) and a PFA needle valve (Fluoroware, MN) was used. All other reactions were carried out in glass reactors, equipped with valves with PTFE stems (Young, London). Solid materials were manipulated inside a drybox (Braun, Munich, Germany), filled with dry argon, with a residual moisture of less than 0.1 ppm.

(c) Instrumentation. (i) Vibrational Spectroscopy. Infrared spectra were recorded at room temperature on a IFS-66v FT spectrometer (Bruker, Karlsruhe, Germany). Two different detectors, together with a KBr/Ge or a 6 μm Mylar/Ge beam splitter, operating in the regions 5000−400 or 650−50 cm^{-1}, respectively, were used. A total of 128 scans were coadded for each spectrum, using an apodized resolution of 2 or 4 cm^{-1}. The samples were crushed between AgBr (Korth, Kiel, Germany), or polyethylene (Cadillac, Hannover, Germany) disks inside the drybox. Raman spectra were recorded at room temperature with a Bruker RFS 100/S FT Raman instrument in the region 5000−80 cm^{-1} with a spectral resolution of 2 cm^{-1}, using the 1064 nm exciting line (~500 mW) of a Nd:YAG laser (Adlas, DPY 301, Lübeck, Germany).

Table 1. Crystallographic Data for $[Rh(CO)_4][Al_2Cl_7]$ and $[Rh(CO)_4][Ga_2Cl_7]$

empirical formula	$C_4Al_2Cl_7O_4Rh$	$C_4Cl_7Ga_2O_4Rh$
fw	517.079	602.54
space group	$\bar{P}1$ (No. 2)	$\bar{P}1$ (No. 2)
a (Å)	9.705(3)	9.649(1)
b (Å)	9.800(2)	9.624(1)
c (Å)	10.268(2)	10.133(1)
α (deg)	76.52(2)	77.38(1)
β (deg)	76.05(2)	76.13(1)
γ (deg)	66.15(2)	65.61(1)
V (Å^3)	856.7(5)	824.4(2)
Z	2	2
D_{calc} (g/cm^3)	2.005	2.427
λ (Å)	0.710 73	0.710 73
T (K)	293	143
linear abs coeff μ (cm^{-1})	21.88	53.3
R1(F_o)[a]	0.0524	0.0358
wR2(F_o^2)[b]	0.1586	0.0792

[a] $R_1 = \Sigma||F_o| - |F_c||/\Sigma|F_o|$. [b] $wR_2 = \sqrt{\Sigma w(F_o^2 - F_c^2)^2/\Sigma w(F_o^2)^2}$.

(ii) NMR Spectroscopy. Preparation of $[Rh(^{13}CO)_x(CO)_{4-x}]^+_{(solv)}$, x ≈ 1, Samples for ^{13}C NMR Studies. A 1 mL volume of a freshly prepared sample of $[Rh(CO)_4]^+$ in HO_3F was transferred to a NMR tube equipped with a rotational symmetrical PTFE valve.[34] Subsequently, ^{13}CO was added in vacuo, until a pressure of 0.5 atm at 25 °C resulted, and then the NMR tube was sealed. ^{13}C NMR spectra were recorded at variable temperatures on a Bruker NMR spectrometer MSL 200, operating at 50.3 MHz.

Preparation of Rh(III) Carbonyl Samples for ^{13}C NMR Studies. ^{13}C NMR spectra were recorded on a Bruker Avance DRX-300 spectrometer, operating at 75.47 MHz, or on a Bruker Avance DRX-500 spectrometer, operating at 125.758 MHz. All reactions were carried out using ^{13}CO during the whole syntheses of the respective species. Solutions of the rhodium carbonyl compounds dissolved in HSO_3F were transferred directly from the reaction vessel via 2 mm o.d. FEP tubes into FEP lining, placed in thin wall NMR glass tubes. The reaction vessel was pressurized by using dry gaseous argon. The NMR signals were referenced against TMS using CD_2Cl_2 films between the FEP lining and the NMR tube as external standard ($\delta(^{13}C) = 54.0$ ppm) and lock. All measurements were carried out at −20 °C.

(iii) Single-Crystal X-ray Diffraction. Diffraction data of $[Rh(CO)_4][Al_2Cl_7]$ were collected at 293 K on a Siemens P4 four-circle diffractometer, whereas those of $[Rh(CO)_4][Ga_2Cl_7]$ were collected at 143 K on a Nonius Kappa CCD-diffractometer. Both data collections utilized graphite-monochromated Mo Kα radiation (λ = 0.71073 Å). The crystallographic data, details on the data collection, and the refinement procedures are found in Table 1. During the data collection of $[Rh(CO)_4][Al_2Cl_7]$, the intensity of two check reflections, which were measured after every 98 reflections, decreased linearly. The data were corrected for this decay, as well as for absorption effects, with the aid of 2 ψ-scans and also for Lorentz and polarization effects. The structure was solved with direct methods (SHELX97)[35] in the space group $\bar{P}1$. Refinements were done by full-matrix least-squares methods on F^2 with anisotropic thermal displacement parameters for all atoms, using the SHELX97 program suite.[35] For $[Rh(CO)_4][Ga_2Cl_7]$, the data collection covered almost the whole sphere of reciprocal space with 3 sets at different κ-angles and 279 frames via ω-rotation ($\Delta/\omega = 1°$) at two times 75 s/frame. The crystal to detector distance

(32) Dudley, F. B.; Cady, G. H. *J. Am. Chem. Soc.* **1959**, *79*, 513.
(33) Zhang, D.; Wang, C.; Mistry, F.; Powell, B.; Aubke, F. *J. Fluorine Chem.* **1996**, *76*, 83.
(34) Gombler, W.; Willner, H. *Int. Lab.* **1984**, *14*, 84.
(35) Sheldrick, G. M.: *SHELXL97-Programs for the Solution and Refinement of Crystal Structures*; University of Göttingen: Göttingen, Germany, 1997.

was 3.4 cm. Crystal decay was monitored by repeating the initial frames at the end of data collection. From the analysis of the duplicate reflections, there was no indication for any decay. The structure was also solved by direct methods and successive difference Fourier syntheses. Refinement applied the full-matrix least-squares methods in SHELX97.[35]

(d) Calculations. The calculations were performed with the GAUSSIAN 98 software package,[36] using density functional theory[37] and employing the three-parameter B3LYB hybrid function,[38] which incorporates the Becke exchange function[39] and the Lee, Yang, Parr correlation function,[40] in combination with 3-21 g* basis set to optimize the molecular geometries to standard convergence criteria. The presented vibrational data are unscaled harmonic wavenumbers and band intensities of the molecules or ions in the gas phase. No ECP was used for Rh. The calculations were done as all-electron calculations.

(e) Synthetic Reactions. (i) Improved Synthetic Route to $[Rh(CO)_5Cl][Sb_2F_{11}]_2$. To a 100 mL PFA round-bottom flask, charged with 50 mg (0.13 mmol) of $[Rh(CO)_2Cl]_2$ and fitted with a PFA adaptor and a PFTE-coated stirring bar, approximately 5 mL of anhydrous HF was added in vacuo, using a stainless steel vacuum line. The reactor was kept at liquid N_2 temperature. Upon warming of the reactor to room temperature, $[Rh(CO)_2Cl]_2$ remained undissolved and no gas evolution (CO) was noted. With the reactor again cooled to −196 °C, 0.9 mmol of F_2 was added, giving rise to a partial F_2 pressure of 0.23 atm at room temperature. After the sample was stirred for a few minutes, the HF phase turned pale yellow. The solid material turned brown and began to cling to the reactor walls. Stirring was continued for a further 2 h, and an additional amount of F_2 (1.3 mmol) was added. After continued stirring for 1 h at room temperature, a brown solid had settled to the bottom, with the supernatant HF phase colorless. With the reactor at liquid N_2 temperature, the excess F_2 was removed in vacuo and about 3 mL of HF and 2 mL of SbF_5 were condensed onto the reaction mixture. Warming of the reaction mixture to room temperature produced a brown, turbid suspension. Further warming to 70 °C resulted in a brown solution after 10 min. After the solution was stirred for a further 30 min, approximately 4.3 mmol of CO was added to give a total pressure of about 1 atm at 25 °C. After the sample was stirred for 20 h at −20 °C, a clear, pale yellow solution resulted, with small amounts of a yellow solid suspended in it. Removal of all volatiles in vacuo yielded a yellow solid which was identified as pure $[Rh(CO)_5Cl][Sb_2F_{11}]_2$ by vibrational spectroscopy and comparison to the published spectrum.[21] The conversion of $[Rh(CO)_2Cl]_2$ into $[Rh(CO)_5Cl][Sb_2F_{11}]_2$ is quantitative.

(ii) *fac*-$Rh(CO)_3(SO_3F)_3$. Inside the drybox, 85 mg (0.219 mmol) of $[Rh(CO)_2Cl]_2$ was added to a carefully dried Raman cell of about 20 mL volume, fitted with a magnetic stirring bar. Subsequently 1.5 mL of HSO_3F and about 0.6 mL of $S_2O_6F_2$ were condensed onto the solid, which dissolved on warming to room temperature to give an orange solution. After the solution was stirred for a further 10 min, the gas phase was removed in vacuo and another 0.5 mL of $S_2O_6F_2$ was added. The resulting mixture was stirred at 80 °C for 24 h, where, according to the vibrational spectra, seemingly oligomeric Rh(III) carbonyl fluorosulfato species had formed, which could not be separated cleanly. After removal of all volatiles in vacuo, about 2 mL of HSO_3F was condensed onto the mixture and 1.6 mmol CO was admitted, to give a partial pressure of 2 atm at 25 °C. Stirring the mixture for several minutes at room temperature resulted in a clear yellow solution of $[Rh(CO)_4]^+_{(solv)}$. After the reactor was cooled to liquid-N_2 temperature, all excess CO was removed in vacuo and 0.6 mL of $S_2O_6F_2$ was added. On warming, vigorous bubbling was noted. After 1 min, before the reaction mixture had warmed to room temperature, the excess $S_2O_6F_2$ and HSO_3F were removed in vacuo and a white, solid material remained, which was subsequently identified by vibrational and ^{13}C NMR spectroscopy as *fac*-$Rh(CO)_3(SO_3F)_3$, again obtained in about 95% yield, with a small amount (∼5%) of a brown byproduct dissolved in HSO_3F.

(iii) $[Rh(CO)_4][Sb_2F_{11}]$. A 100 mg (0.21 mmol) of *fac*-$Rh(CO)_3(SO_3F)_3$ was placed in bulb (A) of a two-bulb PFA reactor, fitted with a stainless steel top. About 1.5 mL of anhydrous HF was added in vacuo, with the bulb A kept at liquid-N_2 temperature. After the mixture was warmed, the color of the white solid changed to dark-orange and the supernatant solution turned pale yellow. After the reaction mixture was stirred for several minutes at room temperature, a red-orange, viscous mass had formed, which was insoluble in HF. In addition CO gas evolution was observed. After the addition of 1.2 mmol of CO to give a partial CO pressure of ∼1 atm at 25 °C, the solid mass began to dissolve in HF and the color changed from orange to yellow. When the process was monitored by Raman spectroscopy, two bands at 2219 (vs) and 2180 cm^{-1} (s) were identified as the Raman-active CO stretches of $[Rh(CO)_4]^+_{(solv)}$.[29,30] After cooling of bulb A to −196 °C and removal of all excess CO in vacuo, 0.5 mL of SbF_5 and 1.2 mmol of CO were added. The mixture was warmed to −40 °C, and HF in the lower part of the reactor bulb became liquid, while solid SbF_5 remained in the upper arm. As soon as the liquid phase came in contact with solid SbF_5, formation of a finely powdered, yellow solid was noted, which subsequently became suspended in HF. After repeated shaking of the reactor by hand, all SbF_5 had been removed from the reactor wall. The resulting mixture was then stirred for 12 h, with the reactor at −20 °C. With the temperature maintained at −20 °C, the supernatant solution containing excess SbF_5 was decanted into bulb B of the double bulb reactor. HF was subsequently condensed back onto the solid, and the washing and decanting process was repeated. After all volatiles were removed in vacuo, the yellow solid residue remaining in the reactor was identified by vibrational analysis as pure $[Rh(CO)_4][Sb_2F_{11}]$ again formed quantitatively.

(iv) Single-Crystal Growth of $[Rh(CO)_4][Al_2Cl_7]$. A glass reactor of about 25 mL volume, fitted with a glass valve with PTFE stem, was, after careful heating in vacuo, charged inside a drybox with 38 mg (0.10 mmol) of $[Rh(CO)_2Cl]_2$ and 54 mg (0.40 mmol) of $AlCl_3$. Both reactants had been finely powdered before mixing. To the reaction mixture, CO was condensed to give at 25 °C a partial pressure of about 1 atm. After the reactor was warmed to room temperature, the color of the reaction mixture changed to bright yellow. The reactor was kept at 25 °C for 3 weeks, and after this time, red needlelike crystals began to grow from the reactor wall toward the center. Raman measurements proved clearly that

(36) Frisch, M. J.; Trucks, G. W.; Schlegel, H. B.; Scuseria, G. E.; Robb, M. A.; Cheeseman, J. R.; Zakrzewski, V. G.; Montgomery, J.; Stratmann, R. E.; Burant, J. C.; Dapprich, S.; Millam, J. M.; Daniels, A. D.; Kudin, K. N.; Strain, M. C.; Farkas, O.; Tomasi, J.; Barone, V.; Cossi, M.; Cammi, R.; Mennucci, B.; Pomelli, C.; Adamo, C.; Clifford, S.; Ochterski, J.; Petersson, G. A.; Ayala, P. Y.; Cui, Q.; Morokuma, K.; Malick, D. K.; Rabuck, A. D.; Raghavachari, K.; Foresman, J. B.; Cioslowski, J.; Ortiz, J. V.; Stefanov, B. B.; Liu, G.; Liashenko, A.; Piskorz, P.; Komaromi, I.; Gomperts, R.; Martin, R. L.; Fox, D. J.; Keith, T.; Al-Laham, M. A.; Peng, C. Y.; Nanayakkara, A.; Gonzalez, C.; Challacombe, M.; Gill, P. M. W.; Johnson, B.; Chen, W.; Wong, M. W.; Andres, J. L.; Gonzalez, C.; Head-Gordon, M.; Replogle, E. S.; Pople, J. A. *GAUSSIAN 98 Rev. A.5*; Gaussian Inc.: Pittsburgh, PA, 1998.
(37) Kohn, W.; Sham, L. J. *Phys. Rev. A* **1965**, *140*, 1133.
(38) Becke, A. D. *J. Chem. Phys.* **1993**, *98*, 5648.
(39) Becke, A. D. *Phys. Rev. A* **1988**, *38*, 3098.
(40) Lee, C.; Yang, W.; Parr, R. G. *Phys. Rev. B* **1988**, *41*, 785.

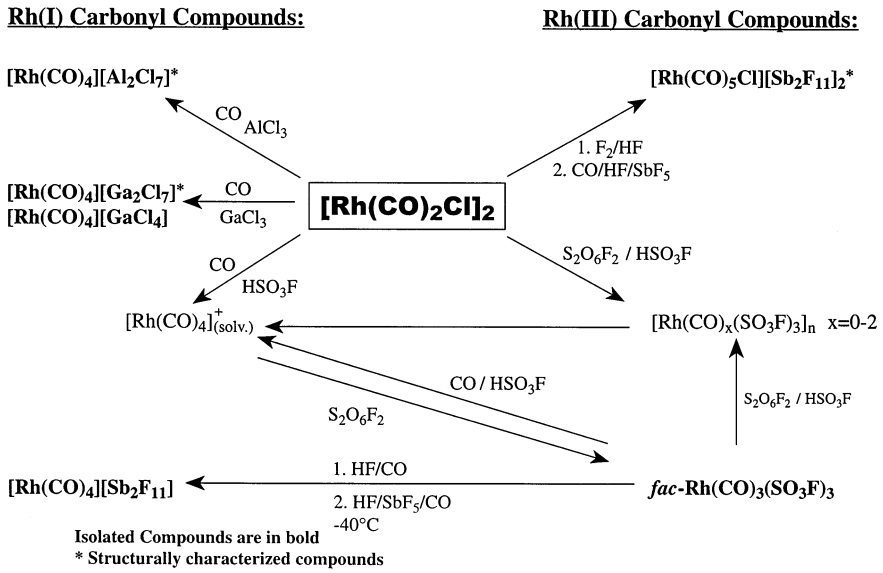

Figure 1. Synthesis of carbonyl compounds of Rh(I) and Rh(III) starting from $[Rh(CO)_2Cl]_2$.

this compound differs from the starting material $[Rh(CO)_2Cl]_2$, but unfortunately, there were no suitable crystals for X-ray diffraction measurements. After a further 1 week, yellow crystallites were noted in a different location, which grew within 2 weeks to yellow prisms with edge lengths of about 1 mm. The yellow crystals were identified by Raman spectroscopy as $[Rh(CO)_4][Al_2Cl_7]$. Suitable crystals were filled inside a drybox under a polarizing microscope into Lindemann glass capillaries and mounted to the goniometer head.

(v) Single-Crystal Growth of $[Rh(CO)_4][Ga_2Cl_7]$. In a round-bottom flask of 100 mL volume, 50 mg (0.13 mmol) of finely ground $[Rh(CO)_2Cl]_2$ was combined inside a drybox with 136 mg (0.77 mmol) of powdered $GaCl_3$. By using a vacuum line, CO was admitted and the CO pressure inside the reactor was adjusted to 1 atm at 25 °C. After the reactor was warmed to room temperature, the mixture began to turn yellow within a few minutes. After several hours, small droplets had formed and melting was noted at the bottom of the flask. Raman spectroscopy revealed the presence of $[Rh(CO)_4][Ga_2Cl_7]$ together with some excess Ga_2Cl_6. After several days, small crystals had formed in the neck of the reactor. Suitable crystals were picked under a polarizing microscope in a stream of dry N_2 and loaded into Lindemann glass capillaries, which in turn were mounted onto the goniometer head.

(vi) $[Rh(CO)_4][GaCl_4]$. In a inverted V-shaped glass reactor with a volume of about 45 mL, 55 mg (0.14 mmol) of $[Rh(CO)_2Cl]_2$ was placed in bulb A and 100 mg (0.57 mmol) of $GaCl_3$ in bulb B. By using a vacuum line, CO was admitted to give inside the reactor a CO pressure of about 0.9 atm at 25 °C. After the reaction mixture was kept at room temperature for several days, small yellow crystallites began to grow at different places inside the reactor, which were examined by Raman spectroscopy. In the neck of bulb B, the spectrum of the product was identical to that of $[Rh(CO)_4][Ga_2Cl_7]$, while those recorded of samples near bulb A showed clearly $[GaCl_4]^-$ as a counteranion of $[Rh(CO)_4]^+$.

Results and Discussion

Synthetic Aspects. (a) General Comments. It has become apparent from the introduction that two important synthetic routes to superelectrophilic[41] metal carbonyl cations and their derivatives,[1−3] reductive and/or solvolytic carbonylation in superacids, may not be appropriate for the syntheses of either Rh(I) or Rh(III) carbonyl complexes. Instead oxidative carbonylations of or halide abstraction from Rh(I) precursors are employed.

A versatile starting material for many syntheses is found to be $[Rh(CO)_2Cl]_2$. The compound is commercially available and known since 1943.[42] Its molecular structure[43] and vibrational spectra[44] are well-known, and $[Rh(CO)_2Cl]_2$ has found in the past extensive use in the syntheses of many organometallic rhodium(I) compounds.[45]

A summary of the synthetic reactions discussed here is shown in Figure 1. With $[Rh(CO)_2Cl]_2$ as precursor, four $[Rh(CO)_4]^+$ salts with different anions are obtained, with two of them, $[Rh(CO)_4][Al_2Cl_7]$ and $[Rh(CO)_4][Ga_2Cl_7]$, structurally characterized. In addition an improved synthetic route to $[Rh(CO)_5Cl][Sb_2F_{11}]_2$ is presented, and the previously unknown compound *fac*-$Rh(CO)_3(SO_3F)_3$ is synthesized in HSO_3F. Furthermore, two additional Rh(III) carbonyl fluorosulfate compounds with different compositions and CO contents are encountered but not isolated. Interconversions of Rh(I) and Rh(III) species in HSO_3F are summarized in Figure 2.

(b) Rhodium(III) Carbonyl Derivatives. The previously reported synthesis of $[Rh(CO)_5Cl][Sb_2F_{11}]_2$[21] involves the oxidative carbonylation of $[Rh(CO)_2Cl]_2$ in $HF-SbF_5$ with SbF_5 as oxidizer. This results in the formation of the adduct $6SbF_3 \cdot 5SbF_5$[28] as a reduced byproduct. While a clean separation of the adduct from the main product is not achieved, due to similar solubilities of both compounds in $HF-SbF_5$, crystals of $[Rh(CO)_5Cl][Sb_2F_{11}]_2$ are picked under a polarizing microscope, on account of their different habit and the structure is subsequently solved.[21] The use of F_2 as external oxidizer, employed in the improved synthesis of $[Rh(CO)_5Cl]$-

(41) Olah, G. A. *Angew. Chem., Int. Ed. Engl.* **1993**, *32*, 767.
(42) Hieber, W.; Legally, H. *Z. Anorg. Allg. Chem.* **1943**, *251*, 96.
(43) Dahl, L. F.; Martell, C.; Wampler, D. L. *J. Am. Chem. Soc.* **1961**, *83*, 1761.
(44) Johnson, B. F. G.; Lewis, J.; Robinson, P. W. *J. Chem. Soc.* **1969**, 2693.
(45) Griffith, W. P. In *The Chemistry of the Rarer Platinium Metals (Os, Ru, Ir, Rh)*; Interscience: New York, 1967; p 384.

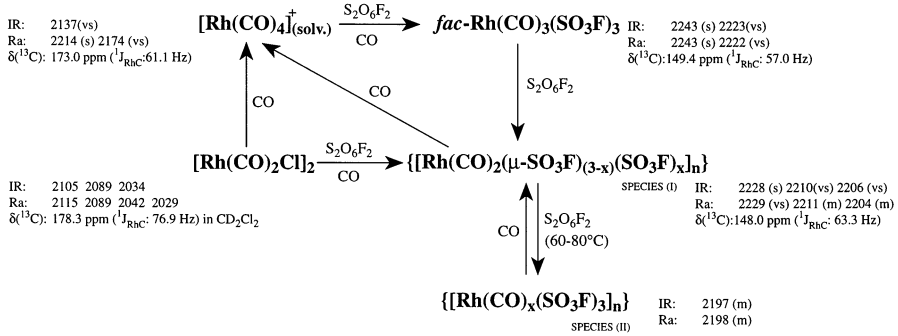

{....} : not cleanly isolated intermediates

Figure 2. Interconversions of Rh(III) and Rh(I) carbonyl fluorosulfate species in HSO_3F and the spectroscopic identification.

$[Sb_2F_{11}]_2$ described here, mandates a separation of the oxidation step from the carbonylation of the oxidized intermediate. The initial step proceeds according to

$$n[Rh(CO)_2Cl]_2 + 2nF_2 \xrightarrow[25\ °C]{HF/F_2} 2[Rh(CO)_2ClF_2]_n \quad (1)$$

The dark brown intermediate, tentatively formulated as $[Rh(CO)_2ClF_2]_n$, is found to be sparingly soluble in aHF (anhydrous HF) but is neither isolated nor characterized. The limited number of completely characterized metal carbonyl fluorides known[46,47] would justify a complete study of this compound; however, this is not intended at this time. The subsequent carbonylation of $[Rh(CO)_2ClF_2]_n$ proceeds cleanly. The dark brown solid dissolves in HF/SbF_5 at 70 °C. The carbonylation of the Rh(III) compound at −20 °C is formulated as

$$[Rh(CO)_2ClF_2]_{(solv)} + 3CO + 4SbF_5 \xrightarrow[-20\ °C]{HF/SbF_2} [Rh(CO)_5Cl][Sb_2F_{11}]_2 \quad (2)$$

The final product is obtained in pure form as a yellow solid. The Raman and IR spectrum of $[Rh(CO)_5Cl][Sb_2F_{11}]_2$ are presented in the Supporting Information as Figure S1 (Raman) and Figure S2 (IR). The vibrational data have been included already in our earlier publication, where the experimental wavenumbers are compared to calculated values.[21]

In contrast to the oxidation with F_2 in aHF, treatment of $[Rh(CO)_2Cl]_2$ in HSO_3F with $S_2O_6F_2$ takes a different course. In a first step, chloride substitution takes place and $ClOSO_2F$ is found as a byproduct, identified by Raman and ^{19}F NMR spectroscopy.[48] Depending on the reaction conditions, two intermediates, labeled **I** and **II** in Figure 2, are obtained. Species **I**, tentatively formulated as $[Rh(CO)_2(\mu\text{-}SO_3F)_{3-x}(SO_3F)_x]_n$, is obtained at 25 °C as a light yellow solid. There are three CO stretches observed, which are IR and Raman active. Their range between 2204 and 2230 cm^{-1} is consistent with expectations[21] for a Rh(III) carbonyl complex. The vibrational spectrum in the SO_3F^- region suggests the presence of bidentate bridging as well as terminal fluorosulfate groups.[18]

Heating a solution of compound **I** in HSO_3F to 60−80 °C in the presence of $S_2O_6F_2$ produces an orange solid, labeled species **II**, which is insoluble in HSO_3F. This compound has a single CO stretch at 2198 cm^{-1}. In the fluorosulfate region, the vibrational spectrum is remarkably similar to that reported for $Rh(SO_3F)_3$,[24] which is also orange in color and almost insoluble in HSO_3F. Since the reaction of $S_2O_6F_2$ with various metal carbonyls is reported to be a useful synthetic route to metal fluorosulfates,[49] it appears likely that $Rh(SO_3F)_3$ is a component of species **II**. While oxidation of $[Rh(CO)_2Cl]_2$ by $S_2O_6F_2$ in HSO_3F appears to be a more facile process than the reported oxidation of rhodium metal,[24] a complete removal of CO from product **II** is not achieved here.

Hence a clean separation and full characterization of the new Rh(III) fluorosulfate compounds is not feasible. As can be seen in Figure 2, species **I** and **II** are readily interconverted in HSO_3F by reaction with either $S_2O_6F_2$ or CO. The carbonylation of species **I** or **II** is found to result in a $2e^-$ reduction and the formation of $[Rh(CO)_4]^+_{(solv)}$.

To complete the oxidative conversions in HSO_3F, illustrated in Figure 2, the previously unknown Rh(III) carbonyl fluorosulfate compound *fac*-$Rh(CO)_3(SO_3F)_3$ can be prepared by a controlled oxidation of $[Rh(CO)_4]^+_{(solv)}$ in HSO_3F by $S_2O_6F_2$. The resulting white solid is isolated and characterized by vibrational and ^{13}C NMR spectroscopy (vide infra). The overall formation reaction is formulated as

$$[Rh(CO)_4]^+_{(solv)} + 2S_2O_6F_2 + SO_3F^- \xrightarrow[-10\ °C]{HSO_3F/S_2O_6F_2} fac\text{-}Rh(CO)_3(SO_3F)_3 + CO_2 + S_2O_5F_2 \quad (3)$$

The exclusive formation of *fac*-$Rh(CO)_3(SO_3F)_3$ from square planar $[Rh(CO)_4]^+_{(solv)}$ appears to reflect the trans-directing ability of CO.[50] According to the overall reaction (eq 3), both a $2e^-$ oxidation (Rh(I) to Rh(III)) by $S_2O_6F_2$ or by two

(46) Doherty, N. N.; Hoffman, N. W. *Chem. Rev.* **1991**, *91*, 553.
(47) Murphy, E. F.; Murugavel, R.; Roesky, H. W. *Chem. Rev.* **1997**, *97*, 3425.
(48) Qureshi, A. M.; Levchuk, L. E.; Aubke, F. *Can. J. Chem.* **1971**, *49*, 35.
(49) DeMarco, R. A.; Shreeve, J. M. *Adv. Inorg. Chem. Radiochem.* **1974**, *16*, 115 and references herein.
(50) Wilkins, R. G. In *Kinetics and Mechanism of Reactions of Transition Metal Complexes*, 2nd ed.; VCH: Weinheim, Germany, 1991; and references therein.

$^{\bullet}SO_3F$ radicals[33,49] and a nucleophilic substitution of CO by SO_3F^- must occur. In the absence of any information on intermediates, nothing meaningful regarding the sequence of both events, the mechanism of oxidation (molecular or radical), or any rearrangement reactions can be said at this time.

A precedent is reported in the fluorination of $Ir_4(CO)_{12}$ by XeF_2 in HF, which results in the formation of *fac*-$Ir(CO)_3F_3$ as a main product, which is structurally characterized by EXAFS.[51] On the other hand, the addition of CO to $Ir(SO_3F)_3$[18] in HSO_3F produces *mer*-$Ir(CO)_3(SO_3F)_3$ as main product, which is also structurally characterized.[19] All these reactions, which illustrate the trans-directing ability of CO[50] as a common feature,[40,51]take place in the Brønsted superacids[11,12] HSO_3F[52] and HF.

Finally, as seen in Figure 2, the direct solvolytic carbonylation of the precursor $[Rh(CO)_2Cl]_2$ in HSO_3F proceeds according to

$$[Rh(CO)_2Cl]_2 + 2HSO_3F + 4CO \xrightarrow[HSO_3F]{\text{1 atm of CO, 25 °C}} 2[Rh(CO)_4]^+_{(solv)} + 2HCl + 2SO_3F^-_{(solv)} \quad (4)$$

and produces the solvated cation $[Rh(CO)_4]^+_{(solv)}$, which is then oxidized by $S_2O_6F_2$ to *fac*-$Rh(CO)_3(SO_3F)_3$. This shortcut would allow one to bypass formation of the intermediates **I** and **II** in a much simpler synthetic approach.

The generation of an isolable Rh(I) carbonyl fluorosulfate of the possible composition $Rh(CO)_3(SO_3F)$ is not achieved by solvent removal from a solution of $[Rh(CO)_4]^+_{(solv)}$ in HSO_3F. Removing the CO atmosphere from the reaction vessel results immediately in the formation of a dark brown, oily solution. A specific, well-defined product is not isolated.

(c) Tetrakis(carbonyl)rhodium(I) **Cation, $[Rh(CO)_4]^+$, in Solid-State Compounds.** The existence of square planar $[Rh(CO)_4]^+$ in solid-state compounds is demonstrated by the recent synthesis of $[Rh(CO)_4][1\text{-}EtCB_{11}F_{11}]$,[16] via carbonylation of the arene complex $[(\eta^6\text{-}C_6H_6)Rh(CO)_2][1\text{-}EtCB_{11}F_{11}]$,[53] and the subsequent structural characterization.[16] In this study a simpler, more direct route of the chloride abstraction from $[Rh(CO)_2Cl]_2$ by the Lewis acids M_2Cl_6 (M = Al, Ga) followed by CO addition is chosen and found to proceed according to

$$[Rh(CO)_2Cl]_2 + 2M_2Cl_6 + 4CO \xrightarrow[\text{1 atm of CO}]{\text{25 °C}} 2[Rh(CO)_4][M_2Cl_7] \quad M = Al, Ga \quad (5)$$

As discussed in the Experimental Section, the reaction is performed in a glass reactor without a solvent. The reactants are found to give crystalline products, suitable for single-crystal X-ray diffraction. Since molecular M_2Cl_6 (M = Al, Ga) is involved in the reaction and is used in a modest excess, $[M_2Cl_7]^-$ (M = Al, Ga) is found as counteranion. If the carbonylation reaction is carried out in a V-shaped reactor, using Ga_2Cl_6 as Lewis acid, the $[Rh(CO)_4]^+$ cation crystallizes with two different counteranions, $[Ga_2Cl_7]^-$ or $[GaCl_4]^-$, depending on the concentration of gallium trichloride (see Experimental Section). The two anions can be clearly identified by Raman spectroscopy due to differences in band positions and intensities.

The use of $AlCl_3$ as Lewis acid has a precedent in the early pioneering studies by Fischer[54,55] and Hieber,[56−58] which have resulted in the discovery of the first homoleptic metal carbonyl cations. They are formed by group 7 metals Mn, Tc, and Re, according to the general equation

$$M(CO)_5X + M'X_3 + CO \xrightarrow[\sim 300 \text{ atm of CO}]{85-100\ ^\circ C} [M(CO)_6][M'X_4] \quad (6)$$

$$M = Mn,[54,55]\ Tc,[58]\ Re;[56,57]\ M' = Al, Fe;\ X = Cl, Br$$

As can be seen, the reaction conditions in these early studies[54−58] are much more severe than the growth of single crystals of $[Rh(CO)_4][M_2Cl_7]$ (M = Al, Ga) from the gas phase at 1 atm of CO and 25 °C described here. It is interesting to note that early attempts to extend this approach to the syntheses of salts with $[M(CO)_6]^{2+}$ (M = Fe, Os) cations had failed.[59] It took almost 30 years until the group 8 cations could be obtained with SbF_5 as Lewis acid.[2,3] The resulting cations are structurally characterized as $[Sb_2F_{11}]^-$ or $[SbF_6]^-$ salts.[23,60]

A plausible pathway for the chloride abstraction from $[Rh(CO)_2Cl]_2$ is suggested by a previous study[61] of the equilibrium

$$[Rh(CO)_2Cl]_2 + 2CO \rightleftharpoons 2Rh(CO)_3Cl \quad (7)$$

Subsequent halide abstraction from monomeric $Rh(CO)_3Cl$ and CO addition are viewed as steps in a facile route to $[Rh(CO)_4][M_2Cl_7]$ (M = Al, Ga).

While the synthesis of $[Rh(CO)_4]^+$ salts by an established organometallic approach[62,63] is accomplished in a straightforward manner, the synthesis of $[Rh(CO)_4][Sb_2F_{11}]$ is a far more challenging task. The halide abstraction from $[Rh(CO)_2Cl]_2$ by SbF_5 is not feasible, on account of the oxidizing prowess of SbF_5. Hence a more circuitous, two step procedure is necessary. The starting material chosen is *fac*-$Rh(CO)_3(SO_3F)_3$, whose synthesis is reported in the preceding part of this section (see also Figure 2).

In a reductive carbonylation, *fac*-$Rh(CO)_3(SO_3F)_3$ is converted in anhydrous HF to $[Rh(CO)_4]^+$ according to

(51) Brewer, S. A.; Brisdon, A. K.; Holloway, J. H.; Hope, E. G.; Peck, L. A.; Watson, P. G. *J. Chem. Soc., Dalton Trans.* **1995**, *18*, 2945.
(52) Thompson, R. C. In *Inorganic Sulphur Chemistry;* Nickless, G., Ed.; Elsevier: Amsterdam, 1968; p 587.
(53) Ivanov, S. V.; Rockwell, J. J.; Polyakov, O. G.; Gaudinski, C. N.; Anderson, O. P.; Solntsev, K. A.; Strauss, S. H. *J. Am. Chem. Soc.* **1998**, *120*, 4224.
(54) Fischer, E. O.; Öfele, K. *Angew. Chem.* **1961**, *73*, 581.
(55) Fischer, E. O.; Fichtel, K.; Öfele, K. *Chem. Ber.* **1962**, *95*, 249.
(56) Hieber, W.; Kruck, T. *Angew. Chem.* **1961**, *73*, 580.
(57) Hieber, W.; Kruck, T. *Z. Naturforsch., B* **1961**, *16*, 709.
(58) Hieber, W.; Lux, F.; Herget, C. *Z. Naturforsch., B* **1965**, *20*, 1159.
(59) Hieber, W.; Frey, V.; John, P. *Chem. Ber.* **1967**, *100*, 1961.
(60) Bernhardt, E.; Bley, B.; Wartchow, R.; Willner, H.; Bill, E.; Kuhn, P.; Sham, I. H. T.; Bodenbinder, M.; Bröchler, R.; Aubke, F. *J. Am. Chem. Soc.* **1999**, *121*, 7188.
(61) Morris, D. E.; Tinker, H. B. *J. Organomet. Chem.* **1973**, *49*, C 53.
(62) Abel, E. W.; Tyfield, S. P. *Adv. Organomet. Chem.* **1970**, *8*, 117.
(63) Beck, W.; Sünkel, K. *Chem. Rev.* **1988**, *88*, 1405.

$$fac\text{-}Rh(CO)_3(SO_3F)_3 + 2CO \xrightarrow[1\ atm\ of\ CO]{HF,\ 25\ °C} [Rh(CO)_4]^+_{(solv)} + SO_3F^- + CO_2 + S_2O_5F_2 \quad (8)$$

with the progress of the reaction monitored by Raman spectroscopy. After cooling of the reaction mixture with liquid nitrogen, excess CO is removed in vacuo and SbF_5 is added to the mixture, together with additional CO. The mixture is warmed first to −40 °C and then to −20 °C according to

$$[Rh(CO)_4]^+_{(solv)} + 2HF + 2SbF_5 \xrightarrow[HF/SbF_5,\ 12\ h]{-40\ to\ -20\ °C,\ 1\ atm\ of\ CO} [Rh(CO)_4][Sb_2F_{11}] + H_2F^+ \quad (9)$$

There are a number of measures taken to ensure formation of pure $[Rh(CO)_4][Sb_2F_{11}]$: (i) The CO atmosphere is seen to stabilize the $[Rh(CO)_4]^+$ cation in solution, prevents CO dissociation, and provides a reducing atmosphere. (ii) An acidic medium is maintained to prevent nucleophilic attack on $[Rh(CO)_4]^+$ by either F^- or SO_3F^-. (iii) The reaction temperature is kept as low as possible to avoid oxidation of $[Rh(CO)_4]^+_{(solv)}$ by SbF_5 and to promote salt formation, which does not seem to require elevated temperatures. (iv) The use of an inverted V-shaped reactor allows removal of excess SbF_5 from the reaction mixture, so that subsequent oxidation of the rhodium(I) carbonyl compound is avoided.

The synthesis of $[Rh(CO)_4][Sb_2F_{11}]$ is important because in most salts of metal carbonyl cations $[Sb_2F_{11}]^-$ is usually the counteranion[1−3] as e.g. in structurally characterized $[Pd(CO)_4][Sb_2F_{11}]_2$.[31] With $[Pd(CO)_4]^{2+}$ and $[Rh(CO)_4]^+$ isoelectronic and isosteric, the effect of a lower complex charge on the conformation of the $[Sb_2F_{11}]^-$ anion can be studied. Unfortunately, the sensitivity of $[Rh(CO)_4]^+$ to oxidation by SbF_5 does not allow much flexibility in temperature, which would be necessary in recrystallization attempts from $HF-SbF_5$.[2,3] Hence we have to rely on vibrational data for the characterization of $[Rh(CO)_4][Sb_2F_{11}]$.

In summary, there is a viable redox chemistry of Rh(III) and Rh(I) carbonyl complexes, which can be exploited in synthetic applications, once the synthetic potential of $[Rh(CO)_2Cl]_2$ is fully recognized.

Structural Aspects. Crystallographic details for $[Rh(CO)_4][Al_2Cl_7]$ and $[Rh(CO)_4][Ga_2Cl_7]$ are found in Table 1. The molecular structure of $[Rh(CO)_4][Ga_2Cl_7]$ is shown in Figure 3, and the packing of $[Rh(CO)_4][Al_2Cl_7]$ is depicted in Figure 4. Selected bond lengths and angles for both salts are listed in Table 2, while in Table 3 structural and spectroscopic properties of the cations in $[Rh(CO)_4][M_2Cl_7]$ (M = Al, Ga), $[Rh(CO)_4][1\text{-}EtCB_{11}F_{11}]$,[16] and $[M(CO)_4][Sb_2F_{11}]_2$ (M = Pd, Pt)[31] are collected and compared.

As can be seen from the crystallographic data in Table 1, both salts $[Rh(CO)_4][Al_2Cl_7]$ and $[Rh(CO)_4][Ga_2Cl_7]$ are isostructural. They crystallize in the triclinic space group $P\bar{1}$ (No.2), and the dinuclear anions $[M_2Cl_7]^-$ have staggered conformations (see Figure 3). In the molecular structure of

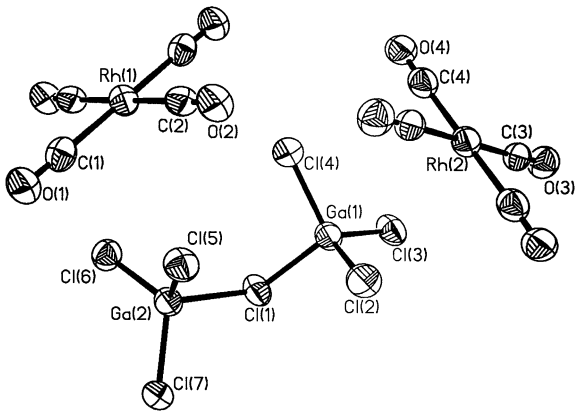

Figure 3. Molecular structure of $[Rh(CO)_4][Ga_2Cl_7]$ with 50% probability thermal ellipsoids shown (ORTEP plot).

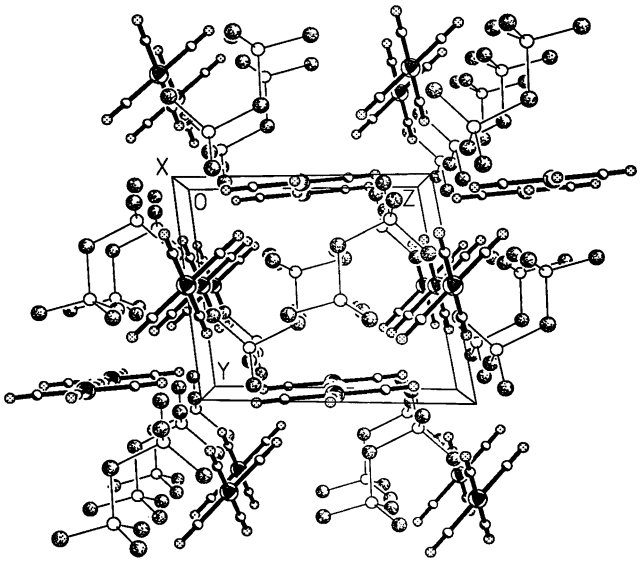

Figure 4. Packing diagram of $[Rh(CO)_4][Al_2Cl_7]$.

$[(Me_6C_6)_3Zr_3Cl_6][Al_2Cl_7]_2$, a related precedent, both a staggered and an eclipsed form of the two $[Al_2Cl_7]^-$ anions are reported.[64]

Of the two isostructural $[Rh(CO)_4][M_2Cl_7]$ salts (M = Al, Ga), the $[Ga_2Cl_7]^-$ salt has surprisingly a slightly smaller unit cell volume *V* by about 3.8% although the square planar $[Rh(CO)_4]^+$ cations have identical bond parameters (see Tables 2 and 3), while for the anions, $[Ga_2Cl_7]^-$, the M−Cl internuclear distances are slightly longer than those in $[Al_2Cl_7]^-$. There are only very few, weak interionic C--Cl contacts to $[Rh(CO)_4]^+$ in both $[M_2Cl_7]^-$ (M = Al, Ga) salts, which are insignificantly shorter than the sum of the van der Waals radii of 3.45 Å.[65]

It hence appears that shrinkage at lower temperatures and more efficient packing of the constituent ions are contributing factors to the observed slightly smaller unit cell volume of $[Rh(CO)_4][Ga_2Cl_7]$ compared to that of $[Rh(CO)_4][Al_2Cl_7]$. Consistent with the assumption of greater packing efficiency, the Ga−Cl−Ga bridge angle in the dinuclear anion is with 112.9(1)° more acute than the corresponding Al−Cl−Al

(64) Stollmaier, F.; Thewalt, U. *J. Organomet. Chem.* **1981**, *208*, 327.
(65) Bondi, A. *J. Phys. Chem.* **1964**, *68*, 441.

Table 2. Selected Internal Bond Parameters for $[Rh(CO)_4][Al_2Cl_7]$ and $[Rh(CO)_4][Ga_2Cl_7]$

	$[Rh(CO)_4][Al_2Cl_7]$	$[Rh(CO)_4][Ga_2Cl_7]$
	Bond Distances (Å)	
Rh(1)−C(1)	1.97(1)	1.968(6)
Rh(1)−C(2)	1.93(1)	1.975(7)
C(1)−O(1)	1.11(1)	1.117(5)
C(2)−O(2)	1.13(1)	1.112(6)
Rh(2)−C(3)	1.97(1)	1.954(6)
Rh(2)−C(4)	1.93(1)	1.957(8)
C(3)−O(3)	1.10(1)	1.134(5)
C(4)−O(4)	1.13(1)	1.129(7)
M(1)−Cl(2)[a]	2.084(4)	2.145(2)
M(1)−Cl(3)	2.097(3)	2.150(1)
M(1)−Cl(4)	2.104(3)	2.162(1)
M(1)−Cl(1)	2.235(3)	2.283(1)
M(2)−Cl(1)	2.278(3)	2.341(2)
M(2)−Cl(5)	2.090(3)	2.134(2)
M(2)-Cl(6)	2.091(4)	2.152(2)
M(2)−Cl(7)	2.092(3)	2.147(1)
	Bond Angles (deg)	
Rh(1)−C(1)−O(1)	179.1(9)	178.5(5)
Rh(1)−C(2)−O(2)	179.5(9)	177.4(5)
Rh(2)−C(3)−O(3)	178.2(9)	176.7(5)
Rh(2)−C(4)−O(4)	178.9(9)	177.8(5)
M(1)−Cl(1)−M(2)	115.5(1)	112.9(1)

[a] M = Al and Ga.

angle of 115.5(1)°, with both anions in an eclipsed conformation. A similarly wide bridge angle of 116.1(4)° is found for the staggered conformation of $[Al_2Cl_7]^-$ in $[(Me_6C_6)_3Zr_3Cl_6][Al_2Cl_7]_2$.[64]

Selected structural (d(M−C), d(C−O)) and vibrational (ν_{CO}, f_{CO}) data for the square planar cations $[Rh(CO)_4]^+$ and $[M(CO)_4]^{2+}$ (M = Pd, Pt)[31] are listed in Table 3 and are compared to calculated data.[31] Also listed are the partial atomic charges for the M−C−O moieties, obtained by DFT methods.[31]

As can be seen, the structural data for the cations in all three $[Rh(CO)_4]^+$ salts are identical within estimated standard deviations and agree well with calculated parameters for $[Rh(CO)_4]^+$(g).[31] The Rh−C distances are all longer than the mean distance d_m (1.846 Å) or the upper quartile q_u value (1.869 Å) from the Cambridge index,[66] based on 238 samples. This reflects the diminished M → CO π-back-bonding, apparent also from the short C−O bond lengths in all three salts. Likewise, the vibrational properties (ν_{CO}, f_{CO}) of $[Rh(CO)_4]^+$ show only very slight anion dependency. Agreement of experimental with calculated data is reasonable, and a complete vibrational analysis of $[Rh(CO)_4]^+$ will be presented in the next section.

In summary all experimental evidence, supported by DFT calculations, points in the case of $[Rh(CO)_4]^+$ to a unipositive homoleptic σ-carbonyl cation with electrophilic carbonyl carbons.[1−3] This conclusion is in harmony with the calculated atomic charges from a natural population analysis[31] with $q_{Rh} = -0.15$, $q_C = 0.56$, and $q_O = -0.28$.[31]

As expected, the increased oxidation state of M in the group 10 salts $[M(CO)_4][Sb_2F_{11}]_2$ (M = Pd, Pt)[31] results in even longer M−C and shorter C−O bond lengths, while $\nu_{CO(avg)}$ is found about 90 cm^{-1} higher than for $[Rh(CO)_4]^+$. There is on account of relativistic effects[67] remarkably little difference in structural data and spectroscopic properties for the isostructural pair $[Pd(CO)_4][Sb_2F_{11}]_2$ and $[Pt(CO)_4][Sb_2F_{11}]_2$, with the unit cell volume for the latter slightly smaller by about 0.4%.[31]

There is another important difference between the $[Rh(CO)_4]^+$ salts and homologous $[M(CO)_4]^{2+}$ (M = Pd, Pt) salts. In $[M(CO)_4][Sb_2F_{11}]_2$ (M = Pd, Pt)[31] as well as in other structurally characterized fluoroantimonate salts of superelectrophilic[41] σ-metal carbonyl cations,[1−3,21,23,60] the distorted $[Sb_2F_{11}]^-$ anions are involved in the formation of extended structures by significant interionic C--F interactions.[1−3] For $[Rh(CO)_4][M_2Cl_7]$ (M = Al, Ga) the dinuclear anions are formed on account of the experimental conditions (see synthesis section) and are only marginally involved in very weak interionic contacts; the $[Rh(CO)_4]^+$ cation can also have the mononuclear $[GaCl_4]^-$ as counteranion. Further evidence for our view comes from a vibrational analysis of $[Rh(CO)_4][Sb_2F_{11}]$ discussed in the next section, where the $[Sb_2F_{11}]^-$ anion has D_{4h} symmetry and is not distorted by interionic contacts to $[Rh(CO)_4]^+$.

For the recently reported $[Rh(CO)_4][1\text{-}EtCB_{11}F_{11}]$, five interionic Rh--F contacts in the range of 3.220(9)−3.588(9) Å are claimed as evidence for "nonclassical" behavior.[16] These contacts, together with an equally weak Rh−H interaction, are claimed to be responsible for the relatively low ν_{CO} value of 2138 cm^{-1} compared to 2162 cm^{-1} reported for the same IR-active vibration in matrix isolated $[Rh(CO)_4]^+$.[68]

We have recalculated the interionic contacts for $[Rh(CO)_4][1\text{-}EtCB_{11}F_{11}]$ from the deposited data for the salt and come to a very different conclusion on two accounts: (i) The reported[16] Rh--F contacts are far too long to be of any significance and are comparable or longer than the estimated sum of the van der Waals radii.[65] On the basis of their length and the atomic charge distribution in $[Rh(CO)_4]^+$ (vide supra), they are judged to be repulsive interactions. (ii) There are however 14 C--F contacts in the range of 2.926−3.155 Å, comparable or slightly shorter than the sum of the van der Waals radii[65] which are not mentioned in ref 16. Since C--F contacts imply a slight electron transfer from the anion to the π^* CO MO's,[2,3] they are most likely responsible for the observed shift of ν_{CO} (E_u) in the solid state compared with matrix data.[61]

In summary, significant interionic or inter- as well as intramolecular contacts to the metal, claimed to be an essential feature of "nonclassical" M−CO bonding,[4] are not observed in σ-carbonyl cations[1−3] and the $[Rh(CO)_4]^+$[16] salts discussed here are no exception regardless of anion. The claim of "nonclassical" behavior for $[Rh(CO)_4][1\text{-}EtCB_{11}F_{11}]$ is based on an erroneous interpretation of the structural data.[16]

Vibrational Spectroscopy. The use of vibrational spectroscopy in this study is limited for a number of reasons:

(i) Our main emphasis is on synthetic aspects, in particular on the development of a viable and synthetically useful redox

(66) Orpen, A. G.; Brammer, L.; Allen, F. H.; Kennard, O.; Watson, P. G.; Taylor, R. *J. Chem. Soc., Dalton Trans.* **1989**, S1.
(67) Pyykkö, P. *Chem. Rev.* **1988**, *88*, 563.
(68) Zhou, M.; Andrews, L. *J. Phys. Chem. A* **1999**, *103*, 7773.

Table 3. Comparison of Structural and Spectroscopic Parameters for Homoleptic D_{4h} Cations $[M(CO)_4]^{n+}$ ($n = 1, 2$)

compd	bond lengths		CO stretching vibratns				^{13}C NMR data		atomic charges[b]			ref
	$d(M-C)_{avg}$ (Å)	$d(C-O)_{avg}$ (Å)	ν_1, ν_6 (Ra) (cm^{-1})	ν_{13} (IR) (cm^{-1})	$\tilde{\nu}(CO)_{avg}$ (cm^{-1})	f_{CO} (10^2 N m^{-1})	$\delta(^{13}C)$ (ppm)	$^1J_{MC}$ (Hz)	q_M	q_C	q_O	
$[Rh(CO)_4][1\text{-Et-}CB_{11}F_{11}]$	1.951(6)	1.118(7)	2215, 2176	2138	2167	19.00[a]	173.5[f]	61.1[f]				16
$[Rh(CO)_4][Al_2Cl_7]$	1.95(1)	1.12(1)	2210, 2167[e]	2137[d]	2163							this work
$[Rh(CO)_4][Ga_2Cl_7]$	1.964(7)	1.123(6)	2209, 2166[e]	2137[d]	2162							this work
$[Rh(CO)_4]^+$(calc)[c]	1.967	1.135	2198, 2150	2119	2147	18.50			−0.15	0.56	−0.28	31
$[Pd(CO)_4][Sb_2F_{11}]_2$	1.992(6)	1.106(6)	2278, 2263	2249	2259	20.63[a]	144.0[g]					31
$[Pd(CO)_4]^{2+}$(calc)[c]	2.016	1.125	2258, 2236	2221	2234	19.86			0.43	0.56	−0.17	31
$[Pt(CO)_4][Sb_2F_{11}]_2$	1.982(9)	1.110(9)	2289, 2267	2244	2261	20.64[a]	137.0[g]	1550				31
$[Pt(CO)_4]^{2+}$(calc)[c]	2.009	1.125	2265, 2237	2216	2234	19.79			0.42	0.55	−0.15	31

[a] Approximation according to Cotton and Kraihanzel. [b] Values in units of e. [c] Calculated data at the BP86/ECP2 level. [d] $[Sb_2F_{11}]^-$ salt. [e] The B_{1g} mode (ν_6) shows clearly a shoulder at higher frequency caused by crystal packing effects. [f] In HSO_3F at −83 °C. [g] MAS at room temperature.

chemistry of Rh(I) and Rh(III) carbonyl compounds in the Brønsted superacids[11,12] anhydrous HF and HSO_3F,[52] with the help of powerful oxidizers such as elemental fluorine[6] and bis(fluorosulfuryl) peroxide, $S_2O_6F_2$.[32,33,50] In this challenging undertaking, vibrational spectroscopy has been very useful in (a) monitoring reactions in situ, primarily by Raman spectroscopy, and (b) identifying intermediates such as e.g. species **I** and **II** shown in Figure 2, which are neither isolated nor more fully characterized.

(ii) One of the isolated and previously structurally characterized rhodium(III) compounds, $[Rh(CO)_5Cl][Sb_2F_{11}]_2$,[21] has been the subject of a complete vibrational analysis of the cation,[21] which includes experimental vibrational data, obtained on the much purer compound, whose synthesis is reported here. The vibrational spectra (Raman, IR) of $[Rh(CO)_5Cl][Sb_2F_{11}]_2$ are presented in the Supporting Information (Figure S1 and S2).

(iii) In a recent, independent study,[69] which deals primarily with the structural characterization of the highly symmetrical (D_{2h}) adduct pyrazine·$2SbF_5$, a comparison of structural and spectroscopic properties of the related high-symmetry (D_{4h}) conformer of the anion $[Sb_2F_{11}]^-$, found in $[Au(CO)_2][Sb_2F_{11}]$[70] and $[H_3F_2][Sb_2F_{11}]$,[71] is reported. The vibrational comparison of $[Sb_2F_{11}]^-$ (D_{4h}) found in $[Au(CO)_2][Sb_2F_{11}]$[70] and in $[Rh(CO)_4][Sb_2F_{11}]$, whose synthesis is described here, is included, together with the results of DFT calculations,[69] as a part of the vibrational characterization of $[Rh(CO)_4][Sb_2F_{11}]$. The vibrational spectra of $[Rh(CO)_4][Sb_2F_{11}]$ are shown as Figure S3 in the Supporting Information.

(iv) A preliminary vibrational analysis of $[Rh(CO)_4]^+$, supported by DFT calculations, has been published recently[31] in the context of the complete vibrational and structural characterization of the related salts $[M(CO)_4][Sb_2F_{11}]_2$, (M = Pd, Pt).[31] The comparison is motivated by the fact that $[Rh(CO)_4]^+$ and $[Pd(CO)_4]^{2+}$ [31] are isoelectronic as well as isostructural. However, in contrast to superelectrophilic[41] square planar $[Pd(CO)_4]^{2+}$ which is only known as the $[Sb_2F_{11}]^-$ salt[31] and forms an extended structure with significant C--F contacts, $[Rh(CO)_4]^+$ is also known with $[1\text{-Et-}CB_{11}F_{11}]^-$,[16] $[M_2Cl_7]^-$ (M = Al, Ga), and $[Sb_2F_{11}]^-$ as counteranions as discussed above, with significant interionic contacts absent.

As seen from the vibrational data for $[Rh(CO)_4][Sb_2F_{11}]$ and $[Rh(CO)_4][M_2Cl_7]$, (M = Al, Ga) listed in Table 4, the observable fundamentals show little anion dependency and agreement with calculated data is good. As previously observed[1−3,21,23,31,60] and discussed, ν_{CO} is in calculations slightly underestimated, usually by about 15−20 cm^{-1}. The Raman spectrum of $[Rh(CO)_4][Al_2Cl_7]$ is shown in Figure 5.

Only a limited number of fundamentals of $[Rh(CO)_4]^+$ are observed for three reasons: (i) For $[Rh(CO)_4][M_2Cl_7]$ (M = Al, Ga), only Raman data are available. (ii) As the bands for the $[M_2Cl_7]^-$ anions (M = Al, Ga) listed in Table 5 and for $[Sb_2F_{11}]^-$ (D_{4h}) in Table 6 show, extensive overlap of anion and cation bands does, in some instances, not permit an unambiguous assignment. (iii) As the calculated intensities for $[Rh(CO)_4]^+$ vibrations show (see Table 4), a substantial number of fundamentals will be unobservable. The calculated wavenumbers also reveal that some fundamentals will be expected to be below 100 cm^{-1}.

With the help of calculated wavenumbers, Raman and IR intensities listed in Table 4, and close analogy to the assignments reported for isoelectronic $[Pd(CO)_4]^{2+}$ and the related cation $[Pt(CO)_4]^{2+}$,[31] a satisfactory vibrational assignment for square planar $[Rh(CO)_4]^+$ is achieved. This assignment is complemented by previously reported force constants,[31] quoted in 10^2 N m^{-1}: $f_{CO(exp)}$, 19.00; $f_{CO(calcd)}$, 18.50; $f_{M-C(calcd)}$, 2.18.

Differences in band positions and force constants between $[Rh(CO)_4]^+$ and $[M(CO)_4]^{2+}$ (M = Pd, Pt)[31] are simply due to the differences in oxidation states of the central metal ions or the complex charges, which cause a shift of all fundamentals for $[M(CO)_4]^{2+}$ (M = Pd, Pt) to higher wavenumbers.[31] Strong interionic F--C contacts for $[M(CO)_4][Sb_2F_{11}]_2$ (M = Pd, Pt)[31] and their absence in $[Rh(CO)_4]^+$ salts have very little effect on the vibrational spectra of the cations.[31] Finally, an IR band at 2162 cm^{-1}, reported in the matrix[60] and attributed to $[Rh(CO)_4]^+$, is considerably higher than the corresponding bands reported here or elsewhere[16,31] for $[Rh(CO)_4]^+$ and should be viewed with some skepticism.

It is interesting to mention that in the Raman spectra of solid $[Rh(CO)_4][M_2Cl_7]$ (M = Al, Ga) there is a shoulder at the B_{1g} CO stretching vibration (ν_6) to higher wavenumbers (see Table 4). This unresolved splitting is thought to be

(69) Sham, I. H. T.; Patrick, B.; v. Ahsen, B.; v. Ahsen, S.; Willner, H.; Thompson, R. C.; Aubke, F. *Solid State Sci.* **2002**, *4*, 1457.
(70) Willner, H.; Schaebs, J.; Hwang, G.; Mistry, F.; Jones, R.; Trotter, J.; Aubke, F. *J. Am. Chem. Soc.* **1992**, *114*, 8972.
(71) Mootz, D.; Bartmann, K. *Angew. Chem., Int. Ed. Engl.* **1988**, *27*, 391.

Table 4. Experimental and Calculated Wavenumbers (cm^{-1}) and Band Intensities for the Cation $[Rh(CO)_4]^+$ (D_{4h}) with Three Different Anions

vibrational modes			BP86/ECP2[a]		$[Rh(CO)_4][Sb_2F_{11}]$		$[Rh(CO)_4][Al_2Cl_7]$		$[Rh(CO)_4][Ga_2Cl_7]$	
			calc	int[b]	expt	int	expt[c]	int	expt[c]	int
ν_1	A_{1g}	ν(CO)	2198	201	2214	s				
ν_6	B_{1g}	ν(CO)	2150	287	2174	vs				
							2167	s	2166	s
ν_{13}	E_u	ν(CO)	2119	**1677**	2137	vs				
ν_{14}	E_u	δ(MCO)	545	**130**	543	s				
ν_8	B_{2g}	δ(MCO)	481	0.1	n.o.		n.o.		n.o.	
ν_4	A_{2u}	δ(MCO)	437	**3.4**	465	m				
ν_{10}	B_{2u}	δ(MCO)	430	i	i					
ν_2	A_{1g}	ν(MC)	423	18.7						
					406[d]	vw	405[d]	w	408[d]	w
ν_7	B_{1g}	ν(MC)	404	1.3						
ν_{15}	E_u	ν(MC)	353	**82**	331	s				
ν_3	A_{2g}	δ(MCO)	320	i	i		i		i	
ν_{12}	E_g	δ(MCO)	316	0.3	306	vw	n.o.[e]		308	vvw
ν_9	B_{2g}	δ(CMC)	91	8.1	n.o.		n.o.		n.o.	
ν_{16}	E_u	δ(CMC)	86	**0.5**	n.o.					
ν_5	A_{2u}	δ(CMC)	54	**0.5**	n.o.					
ν_{11}	B_{2u}	δ(CMC)	30	**i**	i					

[a] Reference 31. Abbreviations: s = strong; m = medium; w = weak; sh = shoulder; v = very; n.o. = not observed; i = inactive mode. [b] Intensities in km mol^{-1} (IR; bold type) or $Å^4$ amu^{-1} (Raman). [c] Only Raman data are available. [d] ν_2 and ν_7 may be accidentally degenerate. [e] Overlap with ν_4 vibration from $[Al_2Cl_7]^-$ (see Table 5).

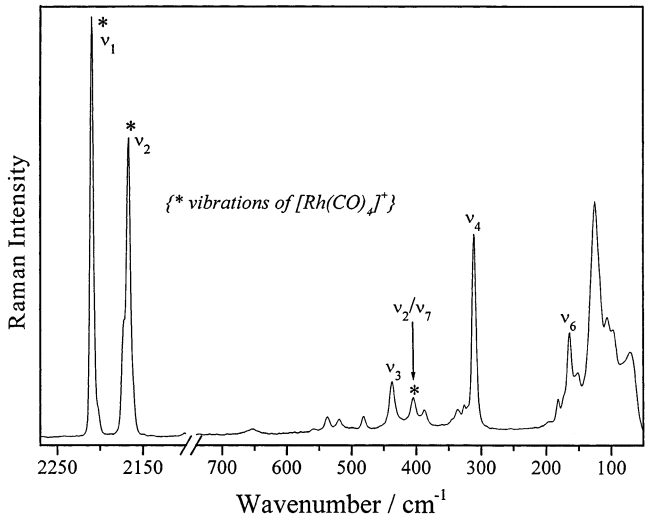

Figure 5. Raman spectrum of $[Rh(CO)_4][Al_2Cl_7]$ (single crystal).

caused by different orientations of the two $[Rh(CO)_4]^+$ cations, in the unit cell, relative to the $[M_2Cl_7]^-$ anions (M = Al, Ga) in the unit cell of the crystal. On the other side, if gallium trichloride is used as Lewis acid in a great excess, the resulting mixture of $[Rh(CO)_4][Ga_2Cl_7]$ in Ga_2Cl_6 becomes liquid at room temperature, due to its low melting point, and the shoulder disappears.

For the related square planar cation $[Ir(CO)_4]^+$, vibrational spectra detected in molten $AlCl_3$ are limited to the CO stretching range. The reported bands at 2216 (A_{1g}), 2170 (B_{1g}), and 2125 (E_u) cm^{-1} compare well to the corresponding bands for $[Rh(CO)_4][Sb_2F_{11}]$ at 2214, 2174, and 2137 cm^{-1}. Similar close correspondence is found for the pairs $[M(CO)_5Cl]^{2+}$ (M = Rh, Ir),[21] $[M(CO)_4]^{2+}$ (M = Pd, Pt)[31] (see Table 3), and $[M(CO)_6]^{2+}$ (M = Ru, Os),[1] all stabilized by $[Sb_2F_{11}]^-$ in isostructural salts.[1−3,21,31]

The vibrational analyses of $[Rh(CO)_4][Al_2Cl_7]$ and $[Rh(CO)_4][Ga_2Cl_7]$ are completed by the listing of calculated and experimental wavenumbers for the $[M_2Cl_7]^-$ (M = Al, Ga) anions in Table 5. For the staggered conformers of C_2 symmetry, found in the molecular structures reported here, 21 nondegenerate (11 A; 10 B) fundamentals are expected in the Raman or the IR spectra. As seen in Table 5, for $[Al_2Cl_7]^-$ 15 bands are detected compared to 12 bands for $[Ga_2Cl_7]^-$, but this number is reduced by two instances of accidental degeneracy and one coincidence with a cation band. For both anions, four fundamentals are expected to fall below 90 cm^{-1} with low intensities. Hence, a satisfactory agreement between results of DFT calculations and experimental observations is achieved for both $[Al_2Cl_7]^-$ and $[Ga_2Cl_7]^-$.

The calculated and experimental wavenumbers for the D_{4h} conformer of $[Sb_2F_{11}]^-$ in $[Rh(CO)_4][Sb_2F_{11}]$ and $[Au(CO)_2][Sb_2F_{11}]$,[70] listed in Table 6, reflect a much simpler situation. While a detailed structural and vibrational analysis of $[Sb_2F_{11}]^-$ (D_{4h}) is reported elsewhere,[69] three salient points are mentioned here: (i) The D_{4h} conformer of $[Sb_2F_{11}]^-$ is easily recognized, because there are in the Sb−F stretching region (800−500 cm^{-1}) 3 IR- and 3 Raman-active bands, which are mutually exclusive. (ii) On increase of the oxidation state of M as e.g. in $[Pd(CO)_4][Sb_2F_{11}]_2$,[31] the electrophilicity of the carbonyl carbon increases, significant C--F contacts are found, the $[Sb_2F_{11}]^-$ distorts to C_{2v} and C_1, and the vibrational spectrum in the Sb−F region becomes more complicated.[31] (iii) The ability of the dioctahedral $[Sb_2F_{11}]^-$ anion to distort by bending of and rotation about the C_4 axis, to facilitate the formation of the C--F interionic contacts, is unique and is documented in more than 10 molecular structures of salts with σ-metal carbonyl cations.[2,3] At the core of this flexibility are weak, linear Sb−F_b−Sb 3c−4e$^-$ bonds which allow rotational as well as bending deformation. The ditetrahedral anion $[M_2Cl_7]^-$ (M = Al, Ga) does not have the same potential as counteranion,[64] and as seen in Table 5, a low-symmetry conformation gives rise to extensive band proliferation even in the absence of significant interionic contacts, as is the case for $[Rh(CO)_4][M_2Cl_7]$ (M = Al, Ga).

Table 5. Experimental and Calculated Wavenumbers (cm^{-1}) and Band Intensities for the Anions $[Al_2Cl_7]^-$ and $[Ga_2Cl_7]^-$

vibrational modes[a]			$[Al_2Cl_7]^-$				$[Ga_2Cl_7]^-$			
			B3LYP	int[b]	expt[c]	int	B3LYP	int[b]	expt[c]	int
ν_{12}	B	$\nu_{as}(MCl_3)$	567	0.8	559	vw	413	2.5	425	vw
ν_1	A	$\nu_{as}(MCl_3)$	567	0.3	559	vw	411	0.8	n.o.[d]	
ν_2	A	$\nu_{as}(MCl_3)$	551	1.5	537	w	401	4.5	397[e]	w
ν_{13}	B	$\nu_{as}(MCl_3)$	546	1.0	519	w	398	2.7		
ν_3	A	$\nu_s(MCl_3)$	438	6.2	438	m	352	23.6	371	vs
ν_{14}	B	$\nu_s(MCl_3)$	392	0.2	388	vw	339	0.9	332	vw
ν_{15}	B	ν_{as}(MClM)	335	0.1	336	vw	291	0.2	289	vw
ν_4	A	ν_s(MClM)	308	10.4	311	s	263	7.0	261	w
ν_5	A	$\delta(MCl_3)$	197	0.4	195	vvw	157	0.3	162	w
ν_{16}	B	$\delta(MCl_3)$	186	1.4	182	w	143	2.1	149	sh
ν_{17}	B	$\delta(MCl_3)$	173	1.5	173	sh	137	1.2	143	vs
ν_6	A	$\delta(MCl_3)$	160	3.0	164	m	131	3.0	139	vs
ν_{18}	B	$\delta(MCl_3)$	154	3.2	152	w	126	2.9	126[f]	m
ν_7	A	$\delta(MCl_3)$	146	1.6	n.o.		125	2.3		
ν_{19}	B	$\delta(MCl_3)$	120	0.4	n.o.		107	0.7	101	sh
ν_8	A	$\delta(MCl_3)$	94	1.7	106	w	82	2.7	n.o.	
ν_9	A	$\delta(MCl_3)$	88	2.1	98	w	75	2.7	n.o.	
ν_{20}	B	$\delta(MCl_3)$	86	0.9	n.o.		73	1.0	n.o.	
ν_{10}	A	δ(MClM)	40	0.2	n.o.		37	0.3	n.o.	
ν_{11}	A	τ(MClMCl)	21	0.0	n.o.		18	0.0	n.o.	
ν_{21}	B	τ(MClMCl)	17	0.0	n.o.		18	0.1	n.o.	

[a] Assuming C_2 symmetry. Abbreviations: see Table 4. [b] Raman intensities in $Å^4$ amu^{-1}. [c] Raman emissions only. [d] ν_1 overlap with ν_2/ν_7 vibration from $[Rh(CO)_4]^+$ cation. [e] ν_2 and ν_{13} may be accidentally degenerated. [f] ν_7 and ν_{18} may be accidentally degenerated.

Table 6. Experimental and Calculated Wavenumbers (cm^{-1}) and Band Intensities for the $[Sb_2F_{11}]^-$ Anion Assuming D_{4h} Symmetry

vibrational modes			B3LYP		$[Rh(CO)_4][Sb_2F_{11}]$		$[Au(CO)_2][Sb_2F_{11}]$	
			calc	int[a]	expt	int	expt	int
ν_{20}	E_u	$\nu_{as}(SbF_{eq})_{ip}$	779	**287**	691	s	689	vs
ν_{16}	E_g	$\nu_{as}(SbF_{eq})_{op}$	775	0.0	n.o.		n.o.	
ν_1	A_{1g}	$\nu(SbF_{ax})_{ip}$	742	5.4	692	m	697	s
ν_6	A_{2u}	$\nu(SbF_{ax})_{op}$	739	**188**	664	**m**	662	sh
ν_7	A_{2u}	$\nu_s(SbF_{eq})_{op}$	702	8.3	n.o.		n.o.	
ν_2	A_{1g}	$\nu_s(SbF_{eq})_{ip}$	697	28.8	651	s	653	vs
ν_{10}	B_{1g}	$\nu_a(SbF_{eq})_{ip}$	679	4.1	598	w	598	m
ν_{14}	B_{2u}	$\nu_a(SbF_{eq})_{op}$	678	i	i		i	
ν_8	A_{2u}	ν_a(SbFSb)	627	**144**	489	**m**	503	**m**
ν_{21}	E_u	δ(SbFSb)	319	**157**	303	**m**	307	**s**
ν_3	A_{1g}	$\delta(SbF_{eq})$	318	0.3	312	vvw	312	sh
ν_{13}	B_{2g}	$\delta(SbF_{eq})$	301	3.6	297	w	293	m
ν_{12}	B_{1u}	$\delta(SbF_{eq})$	299	i	i		i	
ν_{17}	E_g	$\delta(FSbF_{ax})$	294	1.7	273	vw	279	w
ν_{22}	E_u	$\delta(FSbF_{ax})$	283	**46.6**	274	**m**	267	**s**
ν_9	A_{2u}	$\delta(SbF_{eq})$	271	**206**	242	**br**	230	**sh**
					229	w	229	m
ν_{17}	E_g	$\delta(FSbF_{ax})$	294	1.7	273	vw	279	w
ν_{22}	E_u	$\delta(FSbF_{ax})$	283	**46.6**	274	**m**	267	s
ν_9	A_{2u}	$\delta(SbF_{eq})$	271	**206**	242	**br**	230	sh
ν_{18}	E_g	$\delta(SbF_{eq})$	237	3.0	229	w	229	m
ν_{23}	E_u	$\delta(F_{ax}Sb\cdots SbF_{ax})$	200		n.o.		n.o.	
ν_{11}	B_{1g}	$\delta(SbF_{eq})$	158		n.o.		n.o.	
ν_{15}	B_{2u}	$\delta(SbF_{eq})$	154		i		i	
ν_4	A_{1g}	ν_s(SbFSb)	143	0.9	n.o.		131	w
ν_{19}	E_g	$\delta(F_{ax}Sb\cdots SbF_{ax})$	119	0.2	n.o.		n.o.	
ν_5	A_{1u}	$\tau(F_{eq}Sb\cdots SbF_{eq})$	51	i	i		i	
ν_{24}	E_u	δ(SbFSb)	32	**0.1**	n.o		n.o.	

[a] Raman activities in $Å^4$ amu^{-1}; IR activities in km mol^{-1} (bold type). Abbreviations: see Table 4; ip = in phase, op = off phase.

The final example in this section is *fac*-$Rh(CO)_3(SO_3F)_3$, whose synthesis is described here. In the absence of a structural characterization, a vibrational analysis of this compound is essential. Therefore, experimental (Raman, IR, and estimated intensities) and calculated (wavenumbers and Raman and IR band intensities) vibrational data to about 300 cm^{-1} are listed in Table 7. An assignment included here assumes C_{3v} symmetry. The vibrational spectra of *fac*-$Rh(CO)_3(SO_3F)_3$ are shown in Figure 6.

Identification of the compound as *fac*-$Rh(CO)_3(SO_3F)_3$ rests in part on the observation of a single resonance in the ^{13}C NMR spectrum (see Figure 2) ($\delta(^{13}C)$, 149.4 ppm; $^1J_{Rh-C}$, 57.0 Hz) found for solutions in HSO_3F and the observation of two bands in the CO stretching region, ν_1(A) at 2243 (IR and Raman) and ν_{21}(E) at 2223 (IR) or 2222 (Raman) cm^{-1}, with $\nu(CO)_{avg}$ of ~2230 cm^{-1} for the isolated product. These values seem to be at variance with reports for *fac*-$Ir(CO)_3(SO_3F)_3$[19] with 2233 (A), 2156 (E), and $\nu(CO)_{avg.}$ at 2181

Table 7. Experimental and Calculated Vibrational Data for *fac*-$Rh(CO)_3(SO_3F)_3$ to 280 cm^{-1}

exptl data				calcd data		
IR (cm^{-1})	rel int	Ra (cm^{-1})	rel int	B3LYP (cm^{-1})	int IR (km mol^{-1})	int Ra ($Å^4$ amu^{-1})
2243	s	2243	vs	2179.3	124.1	168.5
2223	vs	2222	m	2161.6	180.4	59.2
1392	vs	1391	sh	1398.7	376.2	116.5
		1375	m	1394.3	278.7	109.1
1202	vs, br	1219	m	1161.1	88.9	66.9
		1203	m	1155.5	459.3	20.9
1044	s	1042	w	957.3	15.7	25.2
1009	vs	1001	w	935.5	1155.6	6.6
809	vs	806	w, br	819.0	244.8	9.9
n.o.		834	w	812.7	0.3	2.2
653	m	652	vs	656.2	37.5	49.9
636	m	637	sh	633.1	10.2	15.3
n.o.		599	w	550.8	0.2	1.5
590	s[a]	590	w	550.1	249.2	9.0
548	s	549	sh	506.4	40.5	0.7
556	sh	555	w	501.2	1.6	3.9
529	s	533	vw	487.8	51.5	0.2
500	s	503	w	453.6	60.2	1.6
453	m, br	456	sh	433.7	6.0	3.2
		445	m	431.6	1.9	6.2
431	vw	430	sh	421.0	4.3	2.4
n.o		n.o.		398.7	0.0	0.8
409	w, br)	398	s	376.4	3.8	3.8
n.o		n.o.		355.8	0.3	0.2
372	vw, br	374	s	339.0	1.0	10.2
311	m, br	n.o.		317.9	54.1	0.8
n.o		298	s	289.1	0.5	11.3
b	sh, br	281	s	279.8	16.4	12.0

[a] Band is split into a doublet (593/588 cm^{-1}) due to removal of degeneracy; a very broad and unresolved shoulder to lower frequencies appear at the band at 311 cm^{-1}.

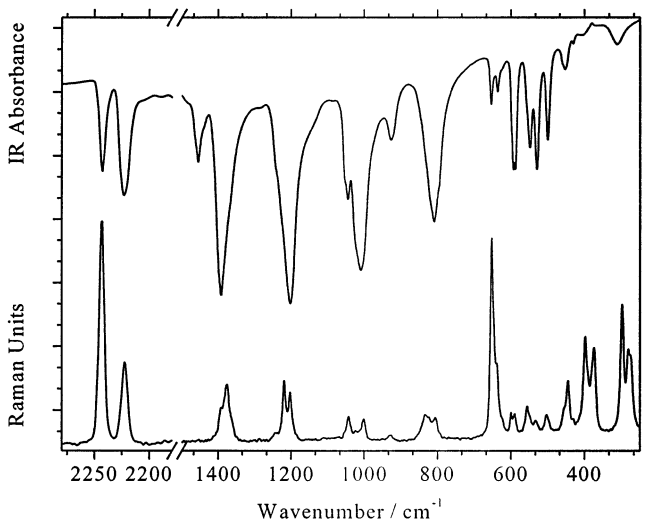

Figure 6. Vibrational spectra of *fac*-$Rh(CO)_3(SO_3F)_3$ (IR, top; Raman, bottom).

cm^{-1}. However in that study, the structurally characterized *mer*-isomer is the main component, with $\nu(CO)_{avg}$ at 2218 cm^{-1}, while the *fac*-$Ir(CO)_3(SO_3F)_3$ is always present in a mixture and the vibrational assignment is tentative and uncertain.[19]

The reported data for $[M(CO)_5Cl]^{2+}$ (M = Rh, Ir)[21] have $\nu(CO)_{avg}$ at 2249 cm^{-1} for the rhodium cation and at 2246 cm^{-1} for its iridium(III) counterpart and at 2268 cm^{-1} for homoleptic $[Ir(CO)_6]^{3+}$.[23] This reflects two general trends: (i) As discussed for $[M(CO)_4]^+$ (M = Rh, Ir), vibrational data for isostructural Rh and Ir carbonyl derivatives differ very little.[2,3] (ii) Replacement of one or more CO ligands in homoleptic metal carbonyl cations by anionic ligands (e.g. Cl^-, SO_3F^-, etc.) results in a gradual decrease of $\nu(CO)_{avg}$.[2,3] Hence the observed band positions for *fac*-$Rh(CO)_3(SO_3F)_3$ agree with expectations, while those reported for *fac*-$Ir(CO)_3(SO_3F)_3$[19] are doubtful, because they are almost 50 cm^{-1} below those of *fac*-$Rh(CO)_3(SO_3F)_3$.

The vibrational spectra in the SO_3F-stretching region (1400−800 cm^{-1}) are consistent with the expectations for a monodentate $-OSO_2F$ group bound to a trivalent metal center in both *fac*-$Rh(CO)_3(SO_3F)_3$ and *mer*-$Ir(CO)_3(SO_3F)_3$.[19] The band distribution with $\nu_{as}(SO_2)$ at 1380 cm^{-1}, $\nu(SO_2)_{sym}$ at 1210 cm^{-1}, ν(SO--M) at 1040−990 cm^{-1}, and ν(SF) at ∼830 cm^{-1} is similar to findings for other structurally characterized metal(III) fluorosulfato complexes such as $[Au(SO_3F)_4]^-$ [15] and $[Au(SO_3F)_3]_2$.[72]

There is more extensive band proliferation in the ν(SO--M) and ν(SF) regions for *mer*-$Ir(CO)_3(SO_3F)_3$[19] because there are two geometrically different $-OSO_2F$ groups in this compound. Finally, for *fac*-$Rh(CO)_3(SO_3F)_3$ there is reasonable agreement between experimental and calculated wavenumbers, which leaves little doubt regarding the proposed structure, even without a conclusive structure determination.

In summary, as demonstrated by us here and elsewhere,[21,31] vibrational spectroscopy in conjunction with DFT calculations is a very powerful structural tool, which is used here in three different ways: (i) For structurally characterized compounds ($[Rh(CO)_4][M_2Cl_7]$ (M = Al, Ga), $[M(CO)_5Cl][Sb_2F_{11}]_2$ (M = Rh, Ir),[21] and $[M(CO)_4][Sb_2F_{11}]_2$ (M = Pd, Pt)[31]) it confirms that the single crystals used in structural studies[21,31] and the bulk compositions are identical. (ii) For these compounds it permits an unambiguous confirmation of the square planar $[M(CO)_4]^-$ cations[31] (M = Rh, Pd, Pt) and the observed anions $[Sb_2F_{11}]^-$ and $[M_2Cl_7]^-$ (M = Al, Ga). (iii) For compounds which are so far not structurally characterized ($[Rh(CO)_4][Sb_2F_{11}]$, *fac*-$Rh(CO)_3(SO_3F)_3$) it confirms both the postulated structures and the composition.

σ-bonded metal carbonyl cations and their derivatives[1−3,19−21,23,31,66,70] are a new class of metal carbonyls. A complete characterization of their salts is essential in our view.

^{13}C NMR Spectroscopy. The use of ^{13}C NMR spectroscopy in the structural analysis of *fac*-$Rh(CO)_3(SO_3F)_3$ has already been discussed. Complementing the structural characterization of $[Rh(CO)_4][M_2Cl_7]$ (M = Al, Ga), the solvated $[Rh(CO)_4]^+$, cation generated from $[Rh(CO)_2Cl]_2$ in a ^{13}C atmosphere is characterized by temperature-dependent ^{13}C NMR in HSO_3F. At ambient temperature (23 °C) a sharp singlet is observed, located at δ_C = 172.5 ppm. Upon cooling, a characteristic line broadening takes place, indicating a dynamic behavior of the $[Rh(CO)_4]^+$ system. After coalescence is passed at −68 °C, a doublet structure is resolved.

(72) Willner, H.; Rettig, S. J.; Trotter, J.; Aubke, F. *Can. J. Chem.* **1991**, *69*, 391.

At the lowest possible temperature (just above the freezing point), a splitting of 61.1 Hz is identified, corresponding to the absolute value of the characteristic rhodium carbon coupling constant $^1J_{RhC}$ in $[Rh(CO)_4]^+$. (It is interesting to note that for *fac*-$Rh(CO)_3(SO_3F)_3$ a value of 57.0 Hz for $^1J_{RhC}$ is found.) A detailed analysis of the NMR data and an explanation for the dynamic nature of the ^{13}C NMR spectrum of $[Rh(CO)_4]^+_{(solv)}$ in HSO_3F will be presented in a further study,[73] which will include additional examples of dynamic ^{13}C NMR in metal carbonyl species in HSO_3F as solvent.

^{13}C NMR data for $[Rh(CO)_2(\mu\text{-}SO_3F)_{3-x}(SO_3F)_x]_n$ (**I**) and *fac*-$Rh(CO)_3(SO_3F)_3$ are listed in Figure 2 and will not be discussed here.

Summary and Conclusions

Rhodium is found to be the first and so far only metal to form thermally stable, fully characterized metal carbonyl cations[1−3] and their derivatives, with rhodium in two distinctly different oxidation states. Starting from dimeric $[Rh(CO)_2Cl]_2$[42−45] halide abstraction by the Lewis acids[11,12] $AlCl_3$ and $GaCl_3$ in the presence of CO allows under mild conditions formation of $[Rh(CO)_4][M_2Cl_7]$ (M = Al, Ga). Both salts are characterized by single crystal X-ray diffraction and a complete vibrational analysis, supported by DFT calculations. Structural and vibrational properties in the CO stretching region of the square planar $[Rh(CO)_4]^+$ (d^8) cation are essentially identical to those reported earlier for $[Rh(CO)_4][1\text{-Et-}CB_{11}F_{11}]$.[16] For $[Rh(CO)_4]^+_{(solv)}$ in HSO_3F, the ^{13}C NMR spectrum is temperature dependent and a dissociative exchange pathway is suggested.[73]

Oxidation of $[Rh(CO)_2Cl]_2$ to Rh(III) carbonyl complexes is achieved by the strongly ionizing and oxidizing solutions of F_2 in the Brønsted superacid HF[11,12] or those of bis(fluorosulfuryl) peroxide, $S_2O_6F_2$,[32,49] in the superacid HSO_3F.[11,12,52] Oxidation of $[Rh(CO)_2Cl]_2$ by F_2 in HF, followed by carbonylation in HF−SbF_5[1−3] in a second step, leads in an improved method to the previously known and structurally characterized $[Rh(CO)_5Cl][Sb_2F_{11}]_2$.[21] Oxidation of $[Rh(CO)_2Cl]_2$ by $S_2O_6F_2$[32,49] in HSO_3F[11,12,52] results in the formation of two, seemingly oligomeric rhodium(III) carbonyl fluorosulfates, which are identified and characterized by vibrational and ^{13}C NMR spectroscopy but not cleanly separated and isolated. Reductive carbonylation of these intermediates produces $[Rh(CO)_4]^+_{(solv)}$ which is subsequently oxidized by $S_2O_6F_2$[32,49] to previously unknown *fac*-$Rh(CO)_3(SO_3F)_3$, characterized by vibrational spectroscopy, DFT calculations, and ^{13}C NMR.

Finally, reductive carbonylation of *fac*-$Rh(CO)_3(SO_3F)_3$ in HF at 25 °C followed by reaction with SbF_5 at −20 °C provides a clean synthetic route to $[Rh(CO)_4][Sb_2F_{11}]$, which is analyzed by vibrational spectroscopy, supported by DFT calculations.

One of the most surprising aspects of the oxidation reactions described here is the resilience of the Rh(III)−CO moieties toward the strongest Brønsted superacids HF[11−14] and HSO_3F[11,12,52] in combination with powerful molecular oxidizing agents such as F_2 and $S_2O_6F_2$.[49]

Acknowledgment. This paper is dedicated to Professor Jeańne M. Shreeve on the occasion of her upcoming birthday. Financial support by the Deutsche Forschungsgesellschaft, the Fonds der Chemischen Industrie, the Natural Sciences and Engineering Research Council of Canada, the Alexander von Humboldt Foundation, and the Heinrich Hertz Stiftung is gratefully acknowledged. Dr. G. Balzer (University Hannover) is thanked for his help in recording ^{13}C NMR spectroscopy. Dr. Stefan von Ahsen is thanked for doing the DFT calculations.

Supporting Information Available: Raman (Figure S1) and IR spectra (Figure S2) of $[Rh(CO)_5Cl][Sb_2F_{11}]_2$ and vibrational spectra of $[Rh(CO)_4][Sb_2F_{11}]$ (Raman, IR; Figure S3). This material is available free of charge via the Internet at http://pubs.acs.org. In addition, complete structure reports are available from Fachinformationszentrum Karlsruhe D-76344 Eggenstein-Leopoldshafen Germany, Hermann von Helmholtz Platz 1. E-mail: crystdata@Fiz.Karlsruhe.de; Fax: int 49-7247-806-666. Deposit numbers: CSD 412960 ($[Rh(CO)_4][Al_2Cl_7]$) and CSD 412961 ($[Rh(CO)_4][Al_2Cl_7]$).

IC0206903

(73) Bach, C.; Bodenbinder, M.; Bley, B.; Willner, H.; Aubke, F.; Hägele, G. *Inorg. Chem.*, manuscript in preparation.